


Cite this: *RSC Adv.*, 2025, 15, 1896

1,2,3-Triazole-tethered fluoroquinolone analogues with antibacterial potential: synthesis and *in vitro* cytotoxicity investigations†

Upendra Kumar Patel,^a Alka,^a Punit Tiwari,^b Ragini Tilak,^b Gaurav Joshi,^c Roshan Kumar^{de} and Alka Agarwal^{id}*^a

The antibacterial efficacy of some newly developed bis- and C3-carboxylic moieties of fluoroquinolone-linked triazole conjugates was studied. Twenty compounds from two different series of triazoles were synthesized using click chemistry and evaluated for their antibacterial activity against a Gram-positive strain, *i.e.* *Enterococcus faecalis* (ATCC29212), and its clinical isolate and a Gram-negative bacterial strain, *i.e.* *Escherichia coli* (ATCC25922), and its clinical isolate. Among the compounds, **7**, **9a**, **9d**, **9i**, **10(a–d)**, and **10i** showed excellent activity with MIC values of up to 6.25 $\mu\text{g mL}^{-1}$, whereas the control ciprofloxacin showed MIC values of up to 12.5 $\mu\text{g mL}^{-1}$ towards the various strains. Cytotoxicity was evaluated against Vero cells (kidney epithelial cells of an African green monkey), and results revealed that compounds **9a**, **9c**, **10g**, **10h**, and **10** are toxic. Molecular docking and MD analysis were performed using the protein structure of *E. coli* DNA gyrase B and further corroborated with an *in vitro* assay to evaluate the inhibition of DNA gyrase. The analysis revealed that compound **10d** was a more potent inhibitor of DNA gyrase compared to ciprofloxacin, which was employed as the positive control.

Received 8th December 2024
Accepted 27th December 2024

DOI: 10.1039/d4ra08643k

rsc.li/rsc-advances

Introduction

Antimicrobial resistance (AMR) poses a severe threat to public health as current antibiotics are becoming less effective in preventing and treating infectious diseases worldwide.¹ Increasing reports of multidrug-resistant (MDR) bacteria pose a significant burden on the healthcare system since MDR infections are associated with increased mortality rates, higher risk of complications, and more extended hospital stays, resulting in substantial financial strain.² *Enterococcus faecalis* (*E. faecalis*) is a commensal bacterium found in the human intestines and a major opportunistic pathogen common in immunocompromised and elderly patients.³ The pathogenesis of *E. faecalis* infection relies in part on its capacity to colonize the gut. Following the disruption of intestinal homeostasis, *E.*

faecalis can overgrow and enter the lymphatic system and bloodstream, crossing the intestinal barrier.⁴ Over 30 years, *E. faecalis* has become a leading cause of healthcare-associated infections worldwide.⁵ It is still a significant health concern and has developed multiple drug resistance, thus causing severe problems in the medical treatment of nosocomial infections,⁶ while *Escherichia coli* (*E. coli*) is one of the most clinically significant Gram-negative bacteria, which is responsible for a wide range of nosocomial infections including urinary tract infections and ventilator-associated pneumonia.⁷ According to the World Health Organization (WHO) classification, *E. coli* is a critical bacterial species resistant to most commercially available drugs.⁸ *Escherichia coli* (*E. coli*) bacteria inhabit the human GI tract and are versatile pathogens. At the same time, *Enterococcus faecalis* (*E. faecalis*) is a facultative, anaerobic, Gram-positive coccus that inhabits the human GI tract.^{9,10} Both *E. coli* and *E. faecalis* are commensal pathogens, and both colonize immediately after birth, thus, they are good representatives of their corresponding phyla.¹¹ From a technical perspective, both species can be easily isolated, grown, and maintained in a laboratory and are frequently used as potential human fecal indicators. Hence, it is urgent to find alternative antimicrobial agents that can reduce the problems of drug resistance in bacteria.

Fluoroquinolones (FQs) are some of the most prominent, widely used classes of synthetic antibacterial agents in treating several infectious diseases. This is because they offer many of the attributes of an ideal antibacterial, combining high potency,

^aDepartment of Medicinal Chemistry, Institute of Medical Sciences, Banaras Hindu University, Varanasi, UP-221005, India. E-mail: agarwal.dralka@gmail.com

^bDepartment of Microbiology, Institute of Medical Sciences, Banaras Hindu University, Varanasi, UP-221005, India

^cDepartment of Pharmaceutical Sciences, Hemvati Nandan Bahuguna Garhwal University (Central University), Dist. Garhwal, Srinagar-246174, Uttarakhand, India

^dDepartment of Microbiology, Central University of Punjab, Ghudda, Bathinda-151401, India

^eDepartment of Microbiology, Graphic Era (Deemed to be University), Clement Town, Dehradun-248002, India

† Electronic supplementary information (ESI) available. CCDC 2345449. For ESI and crystallographic data in CIF or other electronic format see DOI: <https://doi.org/10.1039/d4ra08643k>


broad-spectrum activity, good bioavailability, oral and intravenous formulations, high serum levels, and large distribution volume, indicating good concentrations in different tissues.^{12,13} They play a key role in the treatment of urinary tract infections (UTIs), upper and lower respiratory tract infections (RTI), and sexually transmitted diseases (STDs). Besides their effects in curing skin, soft tissue, gastrointestinal, bones, and joint infections,^{14,15} they exert their bactericidal activity by targeting bacterial DNA gyrase and topoisomerase IV (Topo IV), where they bind to complexes that are formed between DNA and DNA gyrase or Topo IV, forming a ternary complex of DNA enzyme-quinolone. The produced complexes inhibit DNA replication and cell growth and are responsible for the antibacterial activity of fluoroquinolones.¹⁶ However, alone fluoroquinolones cannot control the problems of drug resistance in bacteria, and thus the development of new drugs with effective antibacterial action in a cost-effective manner is necessary. Accordingly, the development of hybrid molecules that inhibit the emergence of drug resistance in bacteria through affinity and efficacy compared to the parent drugs can address these issues.

1,2,3-Triazole is a heterocyclic five-membered ring system possessing three nitrogen and two carbon atoms. Furthermore, 1,2,3-triazole has been a fruitful source of inspiration for medicinal chemists for many years and has attracted our attention due to its synthetic accessibility and diverse inhibitory activities.^{17–19} It can be synthesized *via* the Huisgen 1,3-dipolar cycloaddition of azides and alkynes through copper-catalyzed click reaction.^{20–23} Our literature search showed that the pharmacological effects of 1,2,3-triazole are very alluring and promising for the design of antibacterial agents. Specifically, 1,2,3-triazole conjugated with a wide range of moieties was reported to exhibit potent antibacterial properties.^{24–26}

Previously, we reported a pool of novel fluoroquinolone (ciprofloxacin)-tethered 1,2,3-triazole hybrids with improved antibacterial activity, as shown in Fig. 1. Most of the synthesized conjugates showed enhanced antibacterial activity compared to the parent drug (ciprofloxacin).^{25–27} The study of new hybrid systems (bis and C3-carboxylic group of fluoroquinolone linked triazole hybrids) in which 1,2,3-triazole and fluoroquinolone are combined is an unexplored field of research to date. Thus, the above-mentioned findings encouraged us to investigate the potential synergistic effects of substituted 1,2,3-triazoles and fluoroquinolone scaffolds. Herein, the synthesized hybrids tested against Gram-positive (*E. faecalis*) and Gram-negative (*E. coli*). At the same time, the toxicity of the compounds was evaluated in Vero cells using the MTT assay, where compounds **9a**, **9c**, **10g**, **10h**, and **10i** were found to be toxic. Also, they were further tested using the DNA gyrase assay as a possible target, and molecular docking studies were conducted to investigate their binding mechanisms.

Results and discussion

Chemistry

Bis-fluoroquinolone triazole and fluoroquinolone carboxylic group-linked triazole analogues were synthesized in various steps, as outlined in Scheme 1. In brief, the condensation of 3-chloro-4-

fluoroaniline with diethyl(ethoxymethylene) malonate ester at 100 °C yielded the product (**1**), which underwent a cyclization reaction in diphenyl ether at 250 °C to produce 7-chloro-6-fluoro-4-oxo-1,4-dihydroquinoline-3-carboxylic acid ethyl ester (**2**) in good yield. Consequently, compound (**2**) was alkylated with ethyl bromide using K₂CO₃ in DMF to the corresponding *N*-ethylated product (**3**). The compounds (ethyl 7-chloro-6-fluoro)/(ethyl 7-chloro-1-ethyl-6-fluoro)-4-oxo-1,4-dihydroquinoline-3-carboxylate(**2**)/(**3**) were hydrolyzed into the corresponding acid (**4**)/(**5**) (ethyl 7-chloro-6-fluoro)/(ethyl-7-chloro-1-ethyl-6-fluoro)-4-oxo-1,4-dihydroquinoline-3-carboxylic acid using 2N NaOH solution, respectively. Further, compounds (**4**) and (**5**) were propargylated using propargyl bromide and NaHCO₃ in DMF to the corresponding *N*/*C*-propargylated products (**6**) and (**7**), respectively. Again, the above-propargylated products (**6**) and (**7**) were used to synthesize 1,2,3 compounds **9** and **10(a–i)** *via* click chemistry. All the synthesized compounds were characterized by ¹H, ¹³C NMR, and HRMS.

Biological activity

Antibacterial activity

The antibacterial assay was performed for twenty compounds (fluoroquinolone-triazole hybrids), *i.e.*, **6**, **7**, **9(a–i)**, and **10(a–i)**, which were synthesized from propargylated fluoroquinolones (intermediates) using click chemistry and copper-catalyzed azide-alkyne [3 + 2] cycloaddition. These hybrid compounds, *i.e.*, **6**, **7**, **9(a–i)**, and **10(a–i)**, were tested for their antibacterial property against two-Gram +ve strains, *i.e.* *Enterococcus faecalis* (ATCC 29212) and *Enterococcus faecalis* (clinical isolate) and two-Gram –ve strains, *i.e.*, *Escherichia coli* (ATCC 25922) and *Escherichia coli* (clinical isolate). The MIC results showed that the nature, position, and isomeric effect of the substituents on the phenyl ring significantly impact the antibacterial activity of the prepared compounds (Table 1). According to Table 1, most of the compounds showed greater or equal antibacterial activity in terms of MIC compared to the standard drugs against the investigated strains, *i.e.*, *E. faecalis* (ATCC 29212), *E. faecalis* (clinical isolate), *E. coli* (ATCC 25922) and *E. coli* (clinical isolate) except **9b**, **9c**, **9e**, **9g**, **9h**, **10g**, and **10h**.

Structure–activity relationship

In this part, we summarize the effect of the substituents on the antibacterial activity of the synthesized compounds, as shown in Fig. 2. Compound **6** has an ethyl group on its *N*-atom and propargyl moiety on the carboxylic oxygen of fluoroquinolone, showing good activity against *E. coli* (ATCC 25922) with MIC of $\geq 0.195 \mu\text{g mL}^{-1}$, which is equal to the standard drug. In the other strains, compound **6** was found to be less active than the control with MIC of $1.56 \mu\text{g mL}^{-1}$ against *E. coli* (clinical isolate), *E. faecalis* (ATCC 29212), and *E. faecalis* (clinical isolate) with MIC of $25 \mu\text{g mL}^{-1}$.

Compound **7** is a bis propargylated fluoroquinolone, which showed excellent activity against *E. coli* (clinical isolate) and *E. faecalis* (ATCC 29212) with MIC of $\geq 0.195 \mu\text{g mL}^{-1}$, which is four times greater than that of the standard drug against *E. coli*

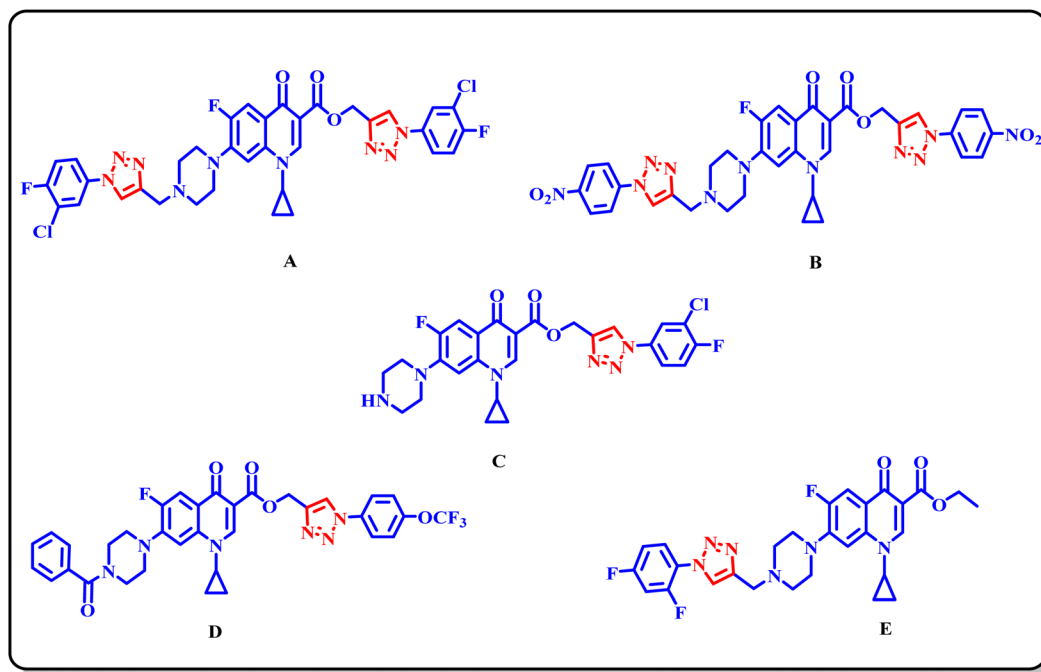


Fig. 1 Structure of some previously reported fluoroquinolone 1,2,3-triazole analogues.

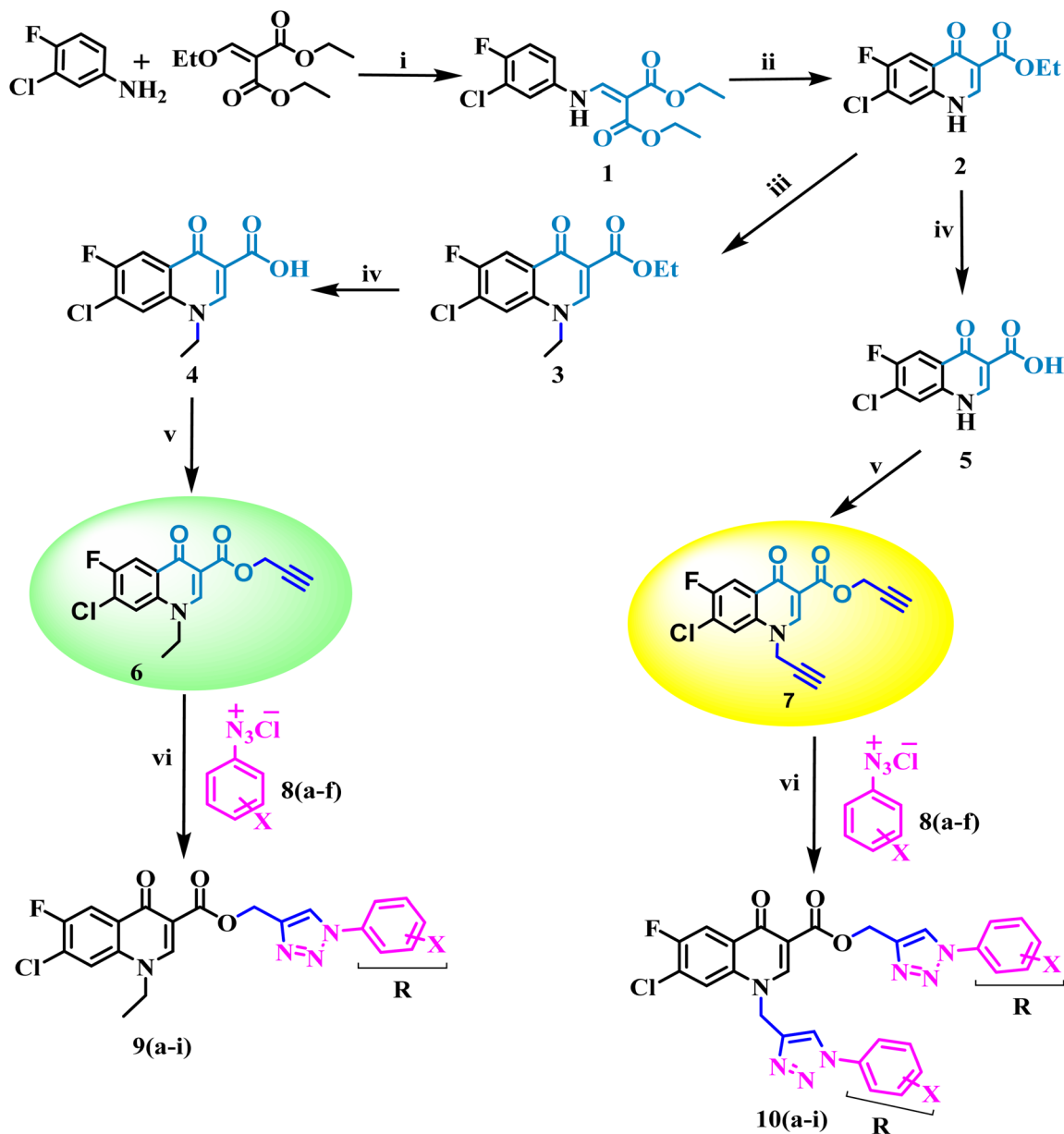
(ATCC 25922) and found to be slightly more active ($\text{MIC } 0.195 \mu\text{g mL}^{-1}$) in comparison to the control drug, while in *E. faecalis* (clinical isolate), it showed equal activity with a $\text{MIC of } 12.5 \mu\text{g mL}^{-1}$, the same as ciprofloxacin showed.

Compound **9a**, a C-3 linked triazole hybrid having 3-Cl and 4-F groups, was found to be four times more active with $\text{MIC of } 0.195 \mu\text{g mL}^{-1}$ in comparison to the standard ($0.781 \mu\text{g mL}^{-1}$) against *E. coli* (clinical isolate). This compound was also found to be equally active as the standard with $\text{MIC of } 0.781 \mu\text{g mL}^{-1}$ against *E. faecalis* (ATCC 29212), while against the other strains, it was found to be active. Compounds **9b** and **9c**, having 3-Cl and 4-OCF₃ groups substituted on the phenyl triazole ring, were found to be less active and showed lower MIC values compared to ciprofloxacin against the respective strains. Compound **9d**, which is a 2,4-difluoro-substituted phenyl triazole ring, was found to be very active ($\text{MIC} \geq 0.195 \mu\text{g mL}^{-1}$) against *E. faecalis* (ATCC 29212) and active against the remaining three strains *i.e.*, *E. coli* (ATCC 25922), *E. coli* (clinical isolate), and *E. faecalis* (clinical isolate) with $\text{MIC} \geq 0.195 \mu\text{g mL}^{-1}$, $\text{MIC} \geq 0.781 \mu\text{g mL}^{-1}$ and $\text{MIC} \geq 12.5 \mu\text{g mL}^{-1}$, which is similar to the standard drug. Compounds **9e**, **9f**, **9g**, and **9h** having 4-Cl, 4-COCH₃, 2-Cl 4-F, and 2,3-dichloro group-substituted phenyl ring, respectively, were all found to have equal activity and were less active than the ciprofloxacin in the tested strains. Compound **9i**, a 4-Cl substituted-phenyl triazole ring, showed potent activity against *E. coli* (ATCC 25922) and *E. coli* (clinical isolate), while it was four times more active ($\text{MIC} \geq 0.195 \mu\text{g mL}^{-1}$) against *E. faecalis* (ATCC 29212) and less active against *E. faecalis* (clinical isolate) in comparison to the standard drug with $\text{MIC} \geq 0.195 \mu\text{g mL}^{-1}$ and $50 \mu\text{g mL}^{-1}$, respectively.

Compounds **10(a-i)** are bis-triazole fluoroquinolone hybrids, as shown in Fig. 2, among which compound **10a**, having 3-Cl, 4-F-substituted benzene triazole, showed the best antibacterial

activity against the tested strains. It showed $\text{MIC of } 0.195 \mu\text{g mL}^{-1}$, which was slightly higher against *E. coli* (ATCC 25922) and four times greater against *E. coli* (clinical isolate) in comparison to ciprofloxacin. Again, the same compound was found to be nearly four times more active ($\text{MIC} \geq 0.195 \mu\text{g mL}^{-1}$) against *E. faecalis* (ATCC 29212), which is similar to compound **9i**, and two times more active with $\text{MIC of } 6.25 \mu\text{g mL}^{-1}$ against *E. faecalis* (clinical isolate) in comparison to ciprofloxacin. Compound **10b** with 3-Cl substituted phenyl triazole showed similar activity as compound **10a** except against *E. coli* (clinical isolate) and *E. faecalis* (clinical isolate), showing $\text{MIC of } \geq 0.195 \mu\text{g mL}^{-1}$, which is nearly four times greater than the control drug, and $\text{MIC of } 12.5 \mu\text{g mL}^{-1}$, a similar value to the control drug. Compound **10c**, a 4-OCF₃-substituted phenyl triazole, was found to be more active against *E. coli* (ATCC 25922) and four times more active against *E. coli* (clinical isolate) in comparison to the standard drug ciprofloxacin with $\text{MIC of } 0.195 \mu\text{g mL}^{-1}$ and $\geq 0.195 \mu\text{g mL}^{-1}$, respectively. The same compound was found to be less active with $\text{MIC of } 0.391 \mu\text{g mL}^{-1}$ against *E. faecalis* (ATCC 29212), while it showed similar activity as the standard drug ($\text{MIC } 12.5 \mu\text{g mL}^{-1}$) against *E. faecalis* (clinical isolate). Compound **10d**, a 2,4-difluoro-containing phenyl triazole hybrid, showed the second most potent activity after **10a** compound, showing similar activity as compound **10a** against *E. coli* (ATCC 25922) and *E. faecalis* (clinical isolate), while it was found to be four times more potent ($\text{MIC } 0.195 \mu\text{g mL}^{-1}$) than the standard drug against *E. faecalis* (ATCC 29212) and *E. coli* (clinical isolate). Compounds **10(e-h)**, having 4-Cl, 4-COCH₃, 2-Cl 4-F, and 2,3-dichloro group-substituted phenyl triazoles, respectively, were found to be equal or less potent than ciprofloxacin against the tested strains. At the same time, compound **10i** was also found to be equal or less active than the standard drug except against *E. coli* (ATCC 25922), which was found to be slightly more





Scheme 1 Schematic representation of the synthesis of fluoroquinolone-triazole analogues.

active with MIC of 0.195 $\mu\text{g mL}^{-1}$. Thus, according to their activity, most of the compounds were found to be active against the investigated strains, while a certain number of compounds were found to be more potent than the standard drugs. Further,

this work can be tuned to obtain useful results, whereas second-generation synthesis, depending on the activity data, is required, and lead compounds should be used in SAR experiments.

Table 1 Antibacterial activity (MIC $\mu\text{g mL}^{-1}$) and cytotoxicity ($\mu\text{g mL}^{-1}$) of compounds 6, 7 & 9–10(a–i)^a

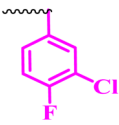
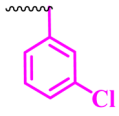
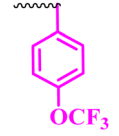
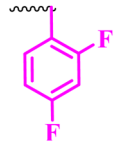
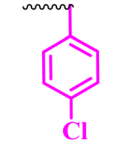
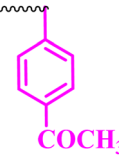
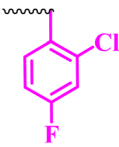
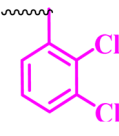
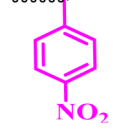
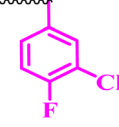
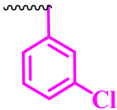
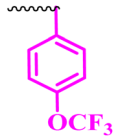
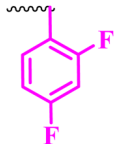
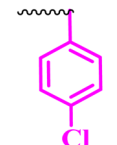
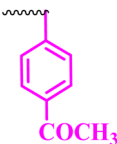
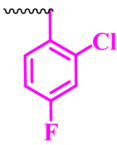
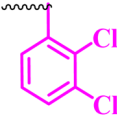
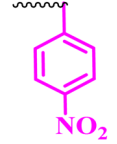
Compound no.	R	Gram + ve strains		Gram –ve strains		CC ₅₀ value ($\mu\text{g mL}^{-1}$)
		<i>E. faecalis</i> (ATCC 29212)	<i>E. faecalis</i> (clinical isolate)	<i>E. coli</i> (ATCC25922)	<i>E. coli</i> (clinical isolate)	
6	—	1.56	25	≥ 0.195	1.56	>100
7	—	≥ 0.195	12.5	0.195	≥ 0.195	>100
9a		0.781	50	12.5	0.195	<100
9b		3.12	100	25	12.5	>100
9c		1.56	50	6.25	3.12	<100
9d		≥ 0.195	12.5	≥ 0.195	0.781	>100
9e		50	100	0.781	12.5	>100
9f		25	50	0.391	0.781	>100
9g		50	50	0.781	6.25	>100
9h		50	100	12.5	25	>100
9i		≥ 0.195	50	0.195	0.781	>100
10a		≥ 0.195	6.25	0.195	0.195	>100



Table 1 (Contd.)

Compound no.	R	Gram + ve strains		Gram –ve strains		CC ₅₀ value ($\mu\text{g mL}^{-1}$)
		<i>E. faecalis</i> (ATCC 29212)	<i>E. faecalis</i> (clinical isolate)	<i>E. coli</i> (ATCC25922)	<i>E. coli</i> (clinical isolate)	
10b		≥ 0.195	12.5	0.195	≥ 0.195	>100
10c		0.391	12.5	0.195	≥ 0.195	>100
10d		0.195	6.25	0.195	≥ 0.195	>100
10e		1.56	50	6.25	0.781	>100
10f		0.781	50	6.25	0.781	>100
10g		25	50	3.12	6.25	<100
10h		3.12	50	6.25	12.5	<100
10i		1.56	12.5	0.195	0.781	<100
Standard	Ciprofloxacin	0.781	12.5	≥ 0.195	0.781	nd
Standard	Chloroquine	nd	nd	nd	nd	>100

^a nd = determined.

Molecular docking studies

We selected the most active compound from the *in vitro* studies, **10d**, and the least active compound, **9a**, for the docking studies to understand the fundamental interactions between the target protein and selected compounds. Both compounds were subjected

to molecular docking studies using the Maestro Schrodinger suite. The protein and ligands were prepared at a pH setting of 7 ± 2 using the Epik module of the Schrodinger software to generate the possible conformers states. The protein used for the docking studies was *E. coli* DNA gyrase B crystal structure in complex with inhibitor 6-fluoro-8-(methylamino)-2-oxo-1,2-dihydroquinoline



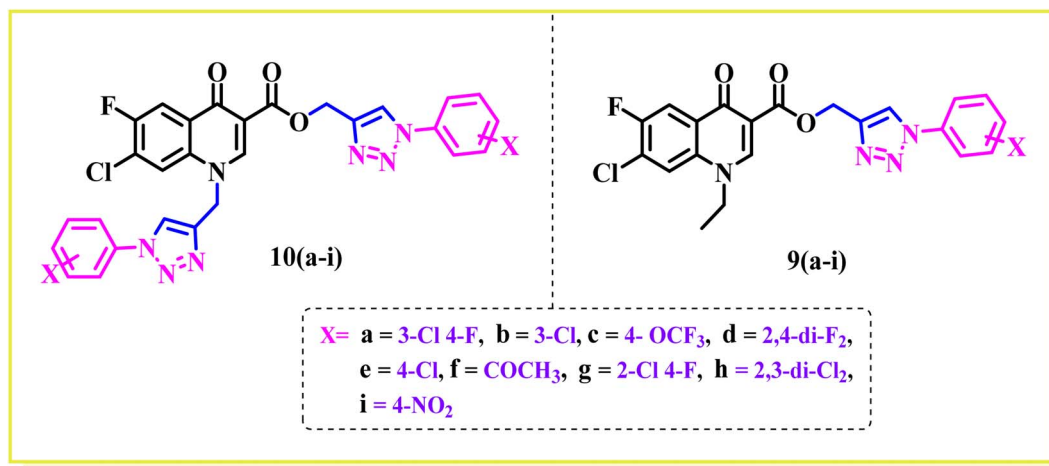


Fig. 2 Structure of fluoroquinolone mono and bis-1,2,3-triazole analogues.

(PDB ID: 7C7N).²⁸ Initially, the docking protocol was validated by calculating the root mean square deviation (RMSD), where the co-crystallized ligand was again redocked to the same cavity (Fig. 3). The docking score of compound **10d** was 7.0 kcal mol⁻¹, which is comparable to that of the standard ciprofloxacin with a value of 7.7 kcal mol⁻¹, and crystallized, as shown in Fig. 4. Compound **10d** interacted with the Asn46, Asp73, and Lys103 amino acid residues. Compound **9a** exhibited a docking score of 4 kcal mol⁻¹.

Molecular dynamic (MD) analysis

Further, to understand the stability of protein-ligand (PL), complex molecular dynamics (MD) studies were performed. Compound **10d** in complex with DNA gyrase B protein (PDB ID: 7C7N) was selected for the MD simulation study. The root-mean-square deviation (RMSD) analysis revealed that the protein showed little fluctuations of around 1.6–2.8 Å throughout the 100 ns simulation time. The

ligand was stable with minimal fluctuation within the range of 1.6–2.4 Å, indicating the ligand remains in the active site of the protein, as shown in Fig. 5(A). Next, the root mean square fluctuation (RMSF) plot was employed to understand the change occurring with time throughout the simulation. The protein and ligand RMSF showed that amino acid residues 100–125 (5.4 Å) [Fig. 5(B)] and 44 atoms (1.75) of the ligand fluctuated, as shown in Fig. 5(C). The PL histogram diagram showed H-bonding interactions with amino acid residues His99 (47%), Ser121 (11%), Asn46 (44%), and Val120 (65%) and π - π interaction with amino acid residues His99 (27%) and Phe104 (10%), as shown in Fig. 5(D and E).

DNA gyrase inhibition assay

We performed the DNA gyrase-based inhibition assay to validate the *in silico* finding of **10d**. The assay was performed in the presence of ciprofloxacin as a positive control. DNA gyrase is

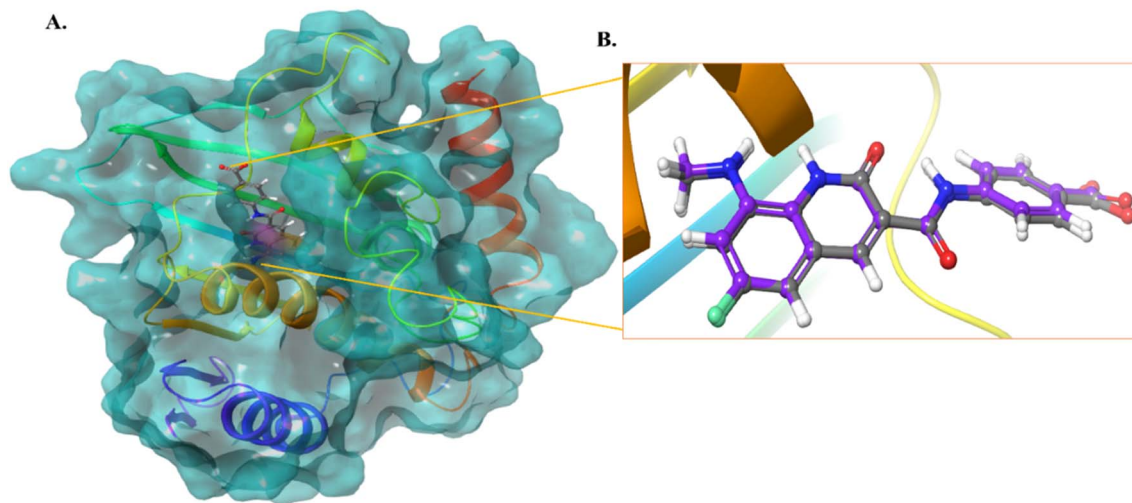


Fig. 3 (A) Protein structure with the co-crystallized ligand. (B) RMSD calculation of the co-crystallized ligand and redocked pose of the co-crystallized ligand (0.1 Å).



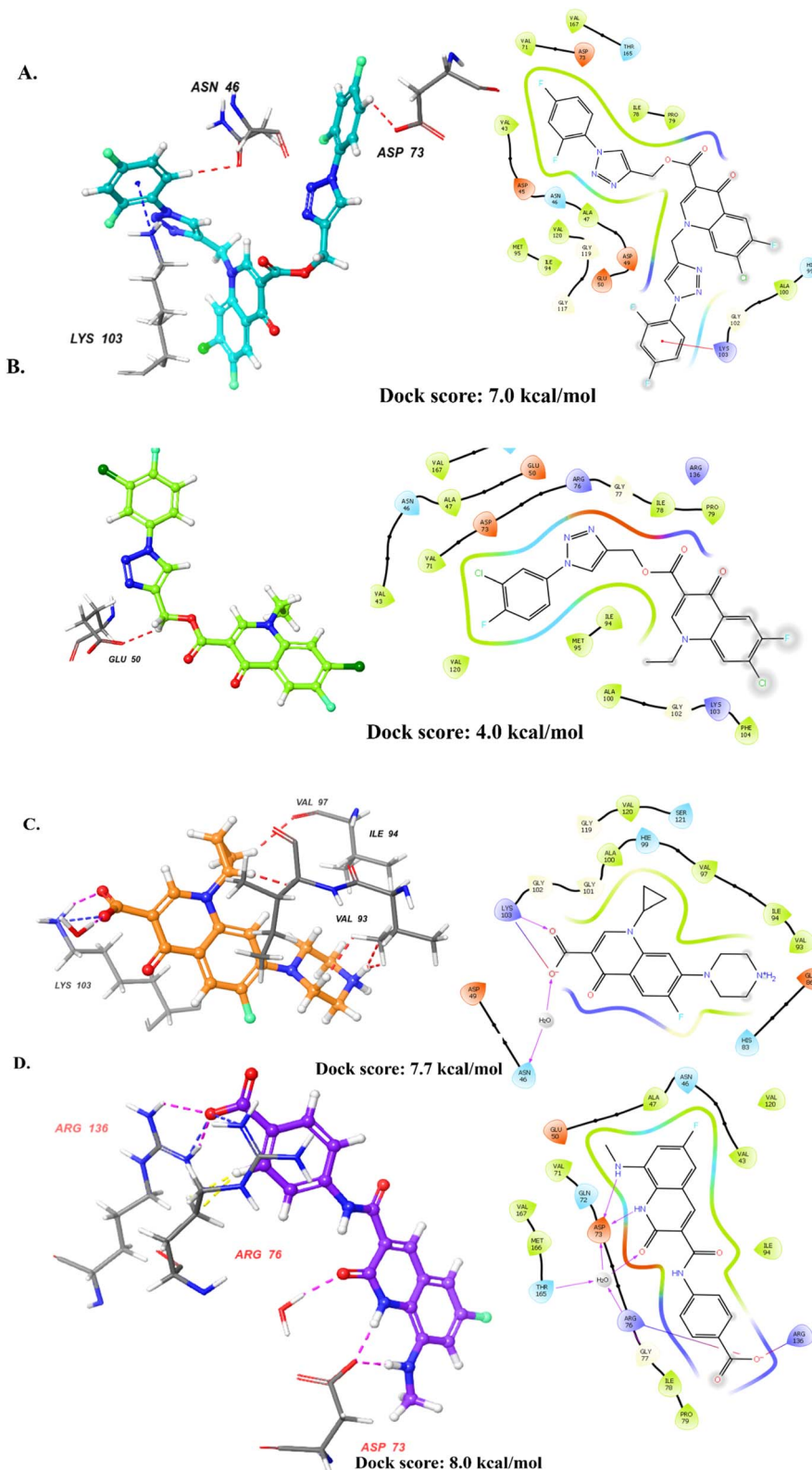


Fig. 4 (A) 3D and 2D interaction of compound 10d. (B) 3D and 2D interaction of compound 9a. (C) 3D and 2D interaction of the compound standard ciprofloxacin. (D) 3D and 2D interaction of the compound co-crystallized ligand.

reported to relieve the negative supercoils in DNA during replication. Usually, upon running agarose gel, the supercoiled form of the DNA molecules tends to migrate faster than the linear form of DNA. Thereby, any decrease in the concentration of the

supercoiled form of DNA and an increase in the relaxed form of the DNA product is linked with DNA gyrase inhibition. The present investigation (Fig. 6) with 9a and 10d at 10 μ M concentration treatment on DNA gyrase inhibition revealed that

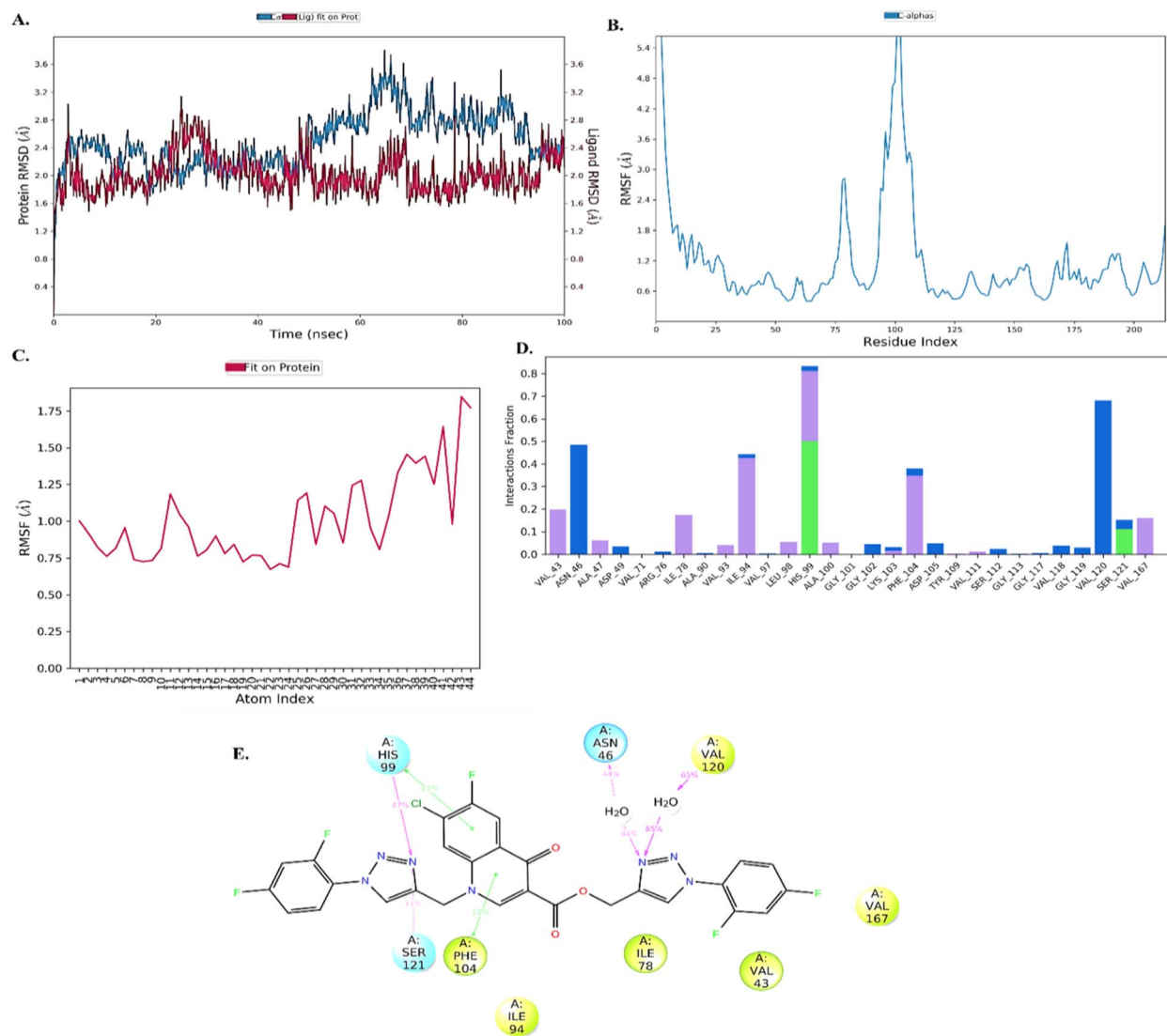


Fig. 5 Molecular dynamic analysis. (A) RMSD analysis of the protein–ligand (**10d**) complex, (B) RMSF analysis of protein, (C) RMSF analysis of the ligand, (D) and protein–ligand histogram analysis and (E) 2D diagram of the ligand with interaction with amino acids.

compound **10d** (as revealed by docking investigations previously) was more potent than **9a**, thus further corroborating the *in silico* findings. The gel image and densitometric plot revealing the decrease in supercoiled DNA are shown in Fig. 6(A and B), respectively.

Cytotoxicity

The cytotoxicity of all the newly synthesized compounds, **6**, **7**, **9(a–i)**, and **10(a–i)**, were evaluated in Vero cells *in vitro* using the published protocol.^{29,30} The results showed that fifteen compounds are free of any considerable cytotoxicity at higher levels of test concentration ($100 \mu\text{g mL}^{-1}$), as shown in Table 1. In contrast, five newly synthesized analogues (**9a**, **9c**, **10g**, **10h** and **10i**) showed toxicity. It is evident from the cytotoxicity results that the functional group position, linkage, nature, and number affect the cytotoxicity of the compounds. For example, compound **9a**, having C-linked monosubstituted triazole with 3-

Cl and 4-F phenyl ring and *N*-ethyl moiety, showed cytotoxicity against Vero cells. Compound **9c** has the same connectivity with *para*-substituted trifluoromethoxy ($-\text{OCF}_3$) phenyltriazole ring also showed cytotoxicity, while the bis triazoles (**10a** and **10c**) of the same compounds did not show any toxicity. In conclusion, we deduced that the *N*-ethyl moiety with monosubstituted triazole having 3-Cl, 4-F, and $-\text{OCF}_3$ -substituted phenyl ring is responsible for the cytotoxicity. Similarly, compound **10g** having bis triazole(C/N-linked triazole) with 2-Cl, 4-F-substituted phenyl ring exhibited cytotoxicity compared to the standard drug at a higher concentration ($100 \mu\text{g mL}^{-1}$). Compounds **10h** and **10i** having 2,3-dichloro and 4- NO_2 groups, respectively, showed toxicity, while monosubstituted triazoles (**9g**, **9h**, and **9i**) of the same compounds were free from cytotoxicity. Thus, we hypothesized that the compounds (**10g**, **10h**, and **10i**) with more functional groups ($-\text{Cl}$, $-\text{F}$, di-Cl, and $-\text{NO}_2$) showed cytotoxicity (Fig. 7).



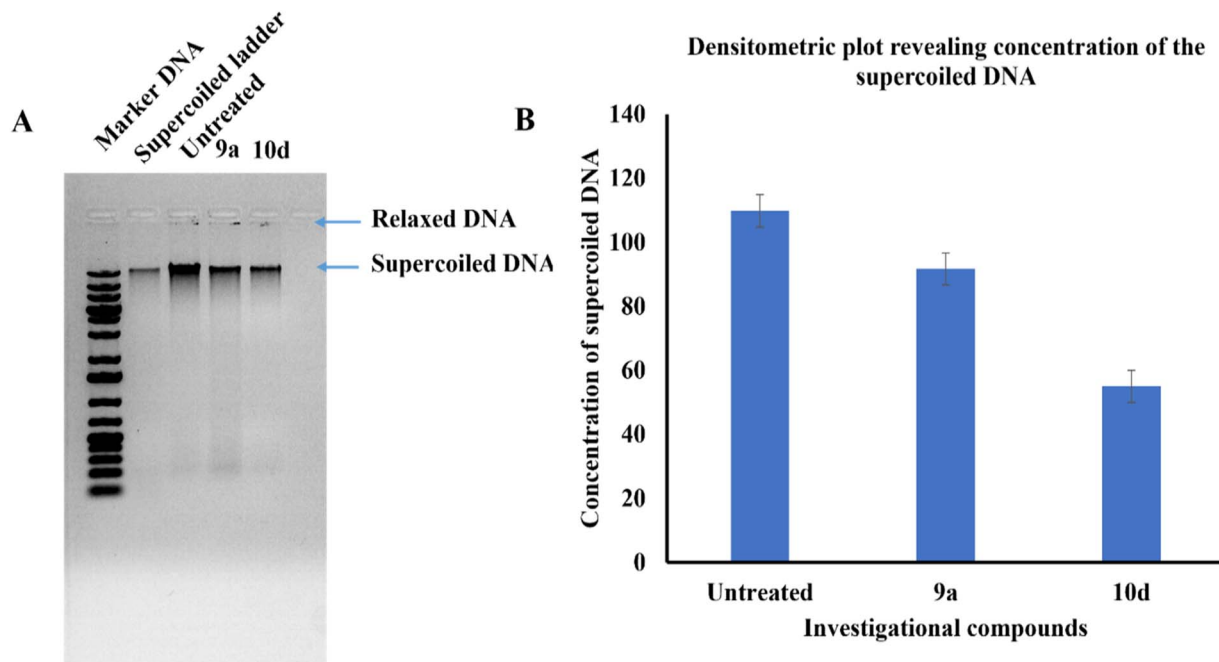


Fig. 6 (A) Agarose gel (inverted image) showing the supercoiled DNA concentration of the treated samples with investigational compounds with respect to untreated DNA. (B) A densitometric plot revealing the concentration of supercoiled DNA which indicates DNA gyrase inhibition.

Experimental

All the chemicals and solvents used in the current study were purchased from E. Merck (India) and Sigma-Aldrich. On pre-coated silica gel 60 F254 (mesh), the reactions during synthesis were monitored *via* thin layer chromatography (TLC), and spots were visualized using UV light. Silica gel (60–120 mesh) was employed for column chromatography. The melting points of all the synthesized compounds were determined using the open capillary method and may be uncorrected. The structural assignments of the synthesized products were based on ^1H NMR, ^{13}C NMR, HRMS, FT-IR, and single-crystal XRD. NMR data were collected using 600 Bruker Avance Neo 600MHz and 400 MHz, JEOL JNM-ECS spectrometer in $\text{DMSO}-d_6$ and CDCl_3 using TMS as an internal standard and Delta software to process the data. In reporting spectra, abbreviations such as s = singlet, bs = broad singlet, d = doublet, dd = doublet of doublets, t = triplet, and m = multiple are used. Mass data was produced using a Bruker Compass spectrometer. X-ray analysis was performed using Rigaku XtaLAB Synergy-i Single Crystal X-ray Diffractometer with a CCD detector (HyPix-Bantam) using graphite mono-chromatized $\text{Cu-K}\alpha$ radiation ($\lambda = 1.54184 \text{ \AA}$).

Method for the synthesis of diethyl-2-(((3-chloro-4-fluorophenyl)amino)methylene)malonate (1)

The synthesis of diethyl 2-(((3-chloro-4-fluorophenyl)amino)methylene)malonate was achieved according to the published procedure.³¹ Briefly, 3-chloro-4-fluoroaniline (24.73 mmol, 3.6 g) and diethyl ethoxymethylenemalonate (27.20 mmol, 5.5 mL) were heated at 100°C for 1.5 h. After this period, the reaction mixture was cooled at room temperature, and ethanol formed during the reaction was removed under vacuum to yield the

crude product. It was purified by recrystallization with *n*-hexane to give the corresponding malonate ester (7.2 g). White solid; yield 7.2 g (92.3%); NMR & mp: reported 1.³¹

Method for the synthesis of ethyl-7-chloro-6-fluoro-4-oxo-1,4-dihydroquinoline-3-carboxylate (2)

The synthesis of ethyl-7-chloro-6-fluoro-4-oxo-1,4-dihydroquinoline-3-carboxylate was achieved *via* the cyclization of malonate ester (1). In short, heating diphenyl ether (50 mL) in an oil bath at 250°C and the above-mentioned malonate ester (1) (20 mmol, 6.3 g) was added slowly. The reaction mixture was refluxed for 1 h with stirring, and a white solid was formed on cooling. The solid was filtered, washed with hexane, and purified through recrystallization from DMF to give 2. White solid; yield 2.15 g (70%); NMR & mp reported 2.³¹

Procedure for the synthesis of ethyl-7-chloro-1-ethyl-6-fluoro-4-oxo-1,4-dihydroquinoline-3-carboxylate (3)

A mixture of compound 2 (4.0 mmol, 1.08 g), K_2CO_3 (20.0 mmol, 2.76 g), and ethyl bromide (20.0 mmol, 2.17 g) in 50 mL DMF was heated at 90°C . After 14 h, the reaction mixture was in ice-cold water to get a white solid precipitate, which was collected by vacuum filtration. The crude products were purified by column chromatography using $\text{CHCl}_3:\text{MeOH}$ (99:1) as the eluent to afford the corresponding N-1 ethyl-substituted quinolones (3).³²

White solid; yield 2.1 g (70.5%); mp: $133\text{--}135^\circ\text{C}$; ^1H NMR (600 MHz, $\text{DMSO}-d_6$) δ : 8.47 (s, 1H, Ar-H), 8.23 (d, $J = 9.0$ Hz, 1H, Ar-H), 7.54 (d, $J = 5.6$ Hz, 1H, Ar-H), 4.39 (q, $J = 7.1$ Hz, 2H, $-\text{OCH}_2$ of $-\text{OCH}_2\text{CH}_3$), 4.24 (q, $J = 7.2$ Hz, 2H, $-\text{NCH}_2$, of $-\text{NCH}_2\text{CH}_3$), 1.57 (t, $J = 7.2$ Hz, 3H, $-\text{CH}_3$ of $-\text{OCH}_2\text{CH}_3$), 1.41 (t, $J = 7.1$ Hz, 3H, $-\text{CH}_3$ of $-\text{NCH}_2\text{CH}_3$); ^{13}C NMR (151 MHz, $\text{DMSO}-$

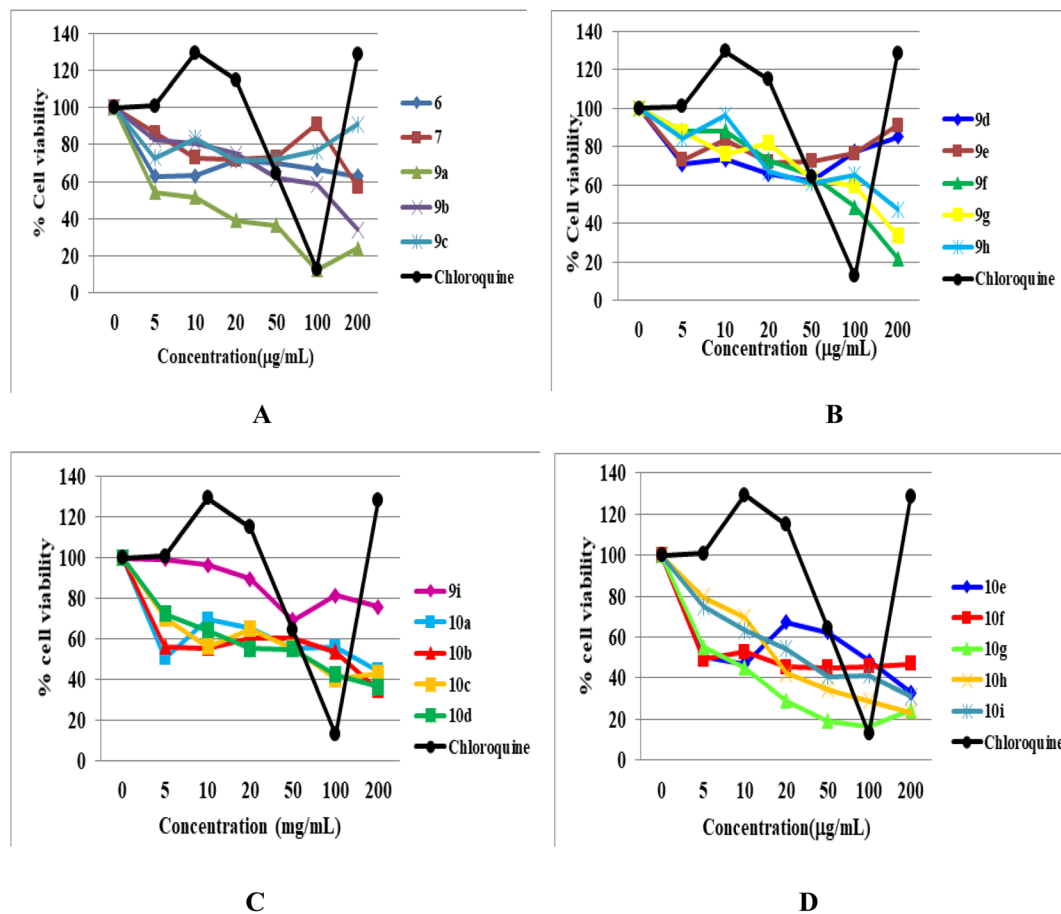


Fig. 7 MTT cytotoxicity. (A) Cell viability of Vero cells treated with compounds **6**, **7**, and **9(a–c)** and chloroquine. (B) Cell viability of Vero cells treated with compounds **9(d–h)** and chloroquine. (C) Cell viability of Vero cells treated with compounds **9i** and **10(a–d)**, and chloroquine. (D) Cell viability of Vero cells treated with compounds **10(e–i)** and chloroquine.

δ : 172.86 (–CO), 165.45 (–CO), 156.39, 154.73, 148.86, 135.46, 129.60 (d, $J = 5.6$ Hz), 127.33 (d, $J = 20.3$ Hz), 118.22, 114.45 (d, $J = 22.5$ Hz), 111.09, 61.20, 49.39, 14.58.

General procedure for the synthesis of 7-chloro-1-ethyl-7-chloro-6-fluoro-4-oxo-1,4-dihydroquinoline-3-carboxylic acid (**4**)/(5)

Compounds **2** and **3** (10.0 mmol, 2.7 g) were refluxed with 2N NaOH (25.0 mL) for 2 h. The mixture was allowed to cool at room temperature and acidified with acetic acid. The solid was filtered, washed with water, and dried under a vacuum. The solid was recrystallized with DMF to give **4** and **5** (2.30 g).³²

7-Chloro-1-ethyl-6-fluoro-4-oxo-1,4-dihydroquinoline-3-carboxylic acid (**4**)

White solid; yield 630 mg (97.83%); mp: 245–247 °C; ^1H NMR (600 MHz, DMSO- d_6) δ : 14.76 (s, 1H, –COOH), 9.07 (s, 1H, Ar–H), 8.44 (s), 8.20 (d, $J = 7.5$ Hz, 1H, Ar–H), 4.61 (s, 2H, –NCH₂, of –NCH₂CH₃), 1.39 (s, 3H, –CH₃ of –NCH₂CH₃); ^{13}C NMR (151 MHz, DMSO- d_6) δ : 176.39 (–CO of –COOH), 166.69 (–CO), 155.37, 153.73, 147.43, 146.13, 138.82, δ 126.05 (d, $J = 20.5$ Hz),

125.98, 124.71 (d, $J = 6.6$ Hz), 123.58, 121.91, 110.85 (d, $J = 22.4$ Hz), 51.65, 16.39.

7-Chloro-6-fluoro-4-oxo-1,4-dihydroquinoline-3-carboxylic acid (**5**)

White solid; yield 1.10 g (91.28%); mp: 287–287 °C; ^1H NMR (600 MHz, DMSO- d_6) δ : 15.26 (s, 1H, –COOH), 8.91 (s, 1H, Ar–H), 8.07 (d, $J = 9.3$ Hz, 1H, Ar–H), 7.99 (d, $J = 6.2$ Hz, 1H, Ar–H); ^{13}C NMR (151 MHz, DMSO- d_6) δ 176.90 (–CO of –COOH), 166.66 (–CO), 155.73, 154.09, 147.10, 138.16, 126.62 (d, $J = 20.7$ Hz), 124.94, 123.20, 111.24 (d, $J = 22.4$ Hz), 107.78.

Procedure for the synthesis of prop-2-yn-1-yl-7-chloro-1-ethyl-6-fluoro-4-oxo-1,4-dihydroquinoline-3-carboxylate (**6**)

Propargylation was performed using a method reported in the literature.³³ To a solution of compound **4** (4.81 mmol, 1.3 g) in dry *N,N*-dimethylformamide (40 mL), in separate round-bottom flasks, 25 mL of NaHCO₃ solution (7.2 mmol, 0.60 g) and (7.2 mmol, 0.86 g) of propargyl bromide were added under vigorous stirring at room temperature. The mixture was allowed to react at 90 °C for 36 h. The progress of the reaction was checked by TLC. After evaporating the solvent, the residue was



purified by column chromatography using a CHCl_3 :MeOH (97 : 3) mixture as the eluent to obtain the desired propargylated product **6**.

Prop-2-yn-1-yl 7-chloro-1-ethyl-6-fluoro-4-oxo-1,4-dihydroquinoline-3-carboxylate (6)

White solid; yield 590 mg (79.65%); mp: 165–167 °C; ^1H NMR (600 MHz, DMSO-d_6) δ : 8.51 (s, 1H, Ar-H), 8.22 (d, J = 9.0 Hz, 1H, Ar-H), 7.55 (d, J = 5.6 Hz, 1H, Ar-H), 4.91 (s, 2H, $-\text{OCH}_2$), 4.25 (q, J = 7.3 Hz, 2H, $-\text{NCH}_2$ of $-\text{NCH}_2\text{CH}_3$), 2.51 (s, 1H, $-\text{C}\equiv\text{CH}$), 1.58 (t, J = 7.3 Hz, 3H, $-\text{CH}_3$ of $-\text{NCH}_2\text{CH}_3$); ^{13}C NMR (151 MHz, DMSO-d_6) δ : 172.35 ($-\text{CO}$), 164.06 ($-\text{CO}$), 156.22, 154.56, 148.88, 135.08, 129.23 (d, J = 5.7 Hz), 127.21 (d, J = 20.2 Hz), 118.01, 114.24 (d, J = 23.0 Hz), 109.70, 77.86, 77.74, 52.03, 49.22, 14.27; IR (KBr) cm^{-1} : 3283, 3062, 1697, 1610, 1486, 1311, 1218, 1172, 1033, 807, 734; HRMS (ESI): anal. calcd. For $\text{C}_{15}\text{H}_{11}\text{ClFNO}_3$, 307.7054 $[\text{M}]^+$; found 308.0491 $[\text{M} + \text{H}]^+$.

Procedure for the synthesis of prop-2-yn-1-yl 7-chloro-6-fluoro-4-oxo-1-(prop-2-yn-1-yl)-1,4-dihydroquinoline-3-carboxylate (7)

Propargylation was done using a method reported in the literature.³³ To a solution of compound **5** (4.1 mmol, 1 g) in dry *N,N*-dimethylformamide (40 mL), in separate round-bottom flasks, 25 mL of NaHCO_3 solution (16.4 mmol, 1.4 g) and (1.2 mmol, 1.95 g) of propargyl bromide were added under vigorous stirring at room temperature. The mixture was allowed to react at 100 °C for 48 h. The progress of the reaction was checked by TLC. After evaporating the solvent, the residue was purified by column chromatography using a CHCl_3 :MeOH (97 : 3) mixture as the eluent to obtain the desired propargylated products **7**.

Prop-2-yn-1-yl-7-chloro-6-fluoro-4-oxo-1-(prop-2-yn-1-yl)-1,4-dihydroquinoline-3-carboxylate (7)

White solid; yield 460 mg (70%); mp: 193–195 °C; ^1H NMR (600 MHz, DMSO-d_6) δ : 8.89 (s, 1H, Ar-H), 8.16 (s, 1H, Ar-H), 8.05 (d, J = 8.8 Hz, Ar-H), 5.36 (s, 2H, $-\text{OCH}_2$), 4.87 (s, 2H, $-\text{NCH}_2$), 3.70 (s, 1H, $-\text{C}\equiv\text{CH}$), 3.57 (s, 1H, $-\text{C}\equiv\text{CH}$); ^{13}C NMR (151 MHz, DMSO-d_6) δ : 171.40 ($-\text{CO}$), 163.17 ($-\text{CO}$), 155.54, 153.89, 149.89, 148.64, 135.53, 128.55 (d, J = 5.2 Hz), 125.53 (d, J = 20.0 Hz), 120.48, 112.73 (d, J = 22.6 Hz), 109.25, 78.79 (d, J = 6.6 Hz), 77.67, 77.20, 51.72, 42.90; IR (KBr) cm^{-1} : 3200, 2125, 1682, 1615, 1481, 1213, 1157, 1028, 755, 549; HRMS (ESI): anal. calcd. For $\text{C}_{16}\text{H}_9\text{ClFNO}_3$, 317.7004 $[\text{M}]^+$; found 318.0347 $[\text{M} + \text{H}]^+$.

General procedure for the synthesis of azides (8a–i)

The azides were synthesized according to the established method.³⁴ Briefly, aniline (1 eq.) was dissolved in 6 N HCl solution (10 mL mmol $^{-1}$ of aniline) at room temperature and cooled to 0 °C and further supplemented with NaNO_2 (1.2 eq.) solution under stirring. After 10 min, sodium azide (1.2 eq.) was added to the reaction mixture at the same temperature under stirring. Again, this mixture was stirred at room temperature for 2–3 h. The reaction was worked up by extraction with ethyl acetate. The organic layer was washed with brine solution and

dried over Na_2SO_4 . After evaporation of the solvent, the crude product (**8a–i**) was pure enough for further reactions.

General procedure for the synthesis of 1,2,3-triazole scaffolds 9–10(a–i)

The triazoles were synthesized according to the literature-reported method.³⁵ In brief, compounds **6** and **7** (1 eq.) and substituted aromatic azide (**9–10(a–i)**, 1.2 eq.) were suspended in *N,N*-dimethylformamide (25 mL mmol $^{-1}$ of alkyne). A solution of sodium ascorbate (0.4 eq. in minimum water) was added, followed by copper(II) sulfate pentahydrate solution (0.2 eq. in minimum water). At room temperature, the heterogeneous mixture was rapidly stirred until alkyne was consumed, and the progress of the reaction was checked by TLC. After completion of the reaction the reaction, the mixture was poured into ice water to get the precipitate and the precipitate was collected by filtration. The required products were purified by column chromatography using CHCl_3 :MeOH (96 : 4) mixture as the eluent.

(1-(3-Chloro-4-fluorophenyl)-1H-1,2,3-triazol-4-yl)methyl 7-chloro-1-ethyl-6-fluoro-4-oxo-1,4-dihydroquinoline-3-carboxylate (9a)

Off white solid; yield 67 mg (86%); mp: 180–182 °C; ^1H NMR (400 MHz, DMSO-d_6) δ : 9.02 (s, 1H, Ar-H), 8.95 (s, 1H, $-\text{C}\equiv\text{CH}$ of triazole), 8.30 (d, J = 6.0 Hz, 1H, Ar-H), 8.23 (dd, J = 6.4, 2.7 Hz, 1H, Ar-H), 8.12 (d, J = 9.3 Hz, 1H, Ar-H), 7.99 (ddd, J = 9.0, 4.1, 2.7 Hz, 1H, Ar-H), 7.72 (t, J = 9.0 Hz, 1H, Ar-H), 5.93 (s, 2H, $-\text{OCH}_2$), 4.32 (q, J = 7.1 Hz, 2H, $-\text{NCH}_2$ of $-\text{NCH}_2\text{CH}_3$), 1.36 (t, J = 7.1 Hz, 3H, $-\text{CH}_3$ of $-\text{NCH}_2\text{CH}_3$); ^{13}C NMR (101 MHz, DMSO-d_6) δ : 172.10 ($-\text{CO}$), 164.75 ($-\text{CO}$), 156.23, 150.92, 143.50, 136.53, 133.86, 129.20, 123.03, 121.58 (d, J = 8.2 Hz), 120.98, 118.62 (d, J = 22.7 Hz), 113.06 (d, J = 22.7 Hz), 110.84, 60.57, 48.50, 14.81; IR (KBr) cm^{-1} : 3093, 2923, 1718, 1610, 1512, 1302, 1223, 1028, 796, 716; HRMS (ESI): anal. calcd. For $\text{C}_{21}\text{H}_{14}\text{Cl}_2\text{F}_2\text{N}_4\text{O}_3$, 479.2648 $[\text{M}]^+$; found 479.0510 $[\text{M} + \text{H}]^+$.

(1-(3-Chlorophenyl)-1H-1,2,3-triazol-4-yl)methyl-7-chloro-1-ethyl-6-fluoro-4-oxo-1,4-dihydroquinoline-3-carboxylate (9b)

Creamy white solid; yield 71 mg (95%); mp: 218–220 °C; ^1H NMR (400 MHz, DMSO-d_6) δ : 8.96 (d, J = 6.9 Hz, 2H, Ar-H, $-\text{C}\equiv\text{CH}$ of triazole), 8.23 (d, J = 6.0 Hz, 1H, Ar-H), 8.02 (dd, J = 17.1, 5.6 Hz, 2H, Ar-H), 7.89 (d, J = 6.9 Hz, 1H, Ar-H), 7.66–7.49 (m, 2H, Ar-H), 5.88 (s, 1H, 2H, $-\text{OCH}_2$), 4.27 (q, J = 7.1 Hz, 2H, $-\text{NCH}_2$ of $-\text{NCH}_2\text{CH}_3$), 1.31 (t, J = 7.1 Hz, 3H, $-\text{CH}_3$ of $-\text{NCH}_2\text{CH}_3$); ^{13}C NMR (101 MHz, DMSO-d_6) δ : 172.10 ($-\text{CO}$), 164.75 ($-\text{CO}$), 150.92, 143.51, 137.93, 136.56, 134.68, 132.12, 129.20, 122.84, 120.73 (d, J = 49.3 Hz), 119.30, 113.07 (d, J = 22.8 Hz), 110.87, 60.56, 48.55, 14.82; IR (KBr) cm^{-1} : 3095, 2929, 1730, 1612, 1485, 1315, 1215, 1162, 1043, 782, 672; HRMS (ESI): anal. calcd. For $\text{C}_{21}\text{H}_{15}\text{Cl}_2\text{FN}_4\text{O}_3$, 461.2744 $[\text{M}]^+$; found 461.0607 $[\text{M} + \text{H}]^+$.

(1-(4-(Trifluoromethoxy)phenyl)-1*H*-1,2,3-triazol-4-yl)methyl-7-chloro-1-ethyl-6-fluoro-4-oxo-1,4-dihydroquinoline-3-carboxylate (9c)

White solid; yield 65 mg (78%); mp: 228–230 °C; ¹H NMR (400 MHz, DMSO-*d*₆) δ: 8.96 (s, 1H, Ar-H), 8.91 (s, 1H, -C=CH of triazole), 8.25 (d, *J* = 5.8 Hz, 1H, Ar-H), 8.01 (dd, *J* = 13.4, 9.1 Hz, 4H, Ar-H), 7.59 (d, *J* = 8.8 Hz, 1H, Ar-H), 5.86 (s, 1H, 2H, -OCH₂), 4.25 (q, *J* = 7.1 Hz, 2H, -NCH₂ of -NCH₂CH₃), 1.29 (t, *J* = 7.0 Hz, 3H, -CH₃ of -NCH₂CH₃); ¹³C NMR (101 MHz, DMSO-*d*₆) δ: 172.10 (-CO), 164.75 (-CO), 153.79 (d, *J* = 5 Hz), 150.92, 143.51, 137.93, 136.56, 134.68, 132.12, 129.14 (d, *J* = 11.5 Hz), 125.84 (d, *J* = 20.3 Hz), 122.84, 120.73 (d, *J* = 49.3 Hz), 119.30, 113.07 (d, *J* = 22.8 Hz), 110.87, 60.56, 48.55, 14.82; IR (KBr) cm⁻¹: 3103, 1728, 1610, 1486, 1270, 1218, 1157, 1038, 801; HRMS (ESI): anal. calcd. For C₂₂H₁₅ClF₄N₄O₄, 510.8296 [M]⁺; found 511.0821 [M + H]⁺.

(1-(2,4-Difluorophenyl)-1*H*-1,2,3-triazol-4-yl)methyl-7-chloro-1-ethyl-6-fluoro-4-oxo-1,4-dihydroquinoline-3-carboxylate (9d)

Off-white solid; yield 59 mg (78%); mp: 218–220 °C; ¹H NMR (400 MHz, DMSO-*d*₆) δ: 8.95 (s, 1H, Ar-H), 8.71 (s, 1H, -C=CH of triazole), 8.31 (d, *J* = 5.8 Hz, 1H, Ar-H), 7.99 (d, *J* = 9.1 Hz, 1H, Ar-H), 7.84 (dd, *J* = 14.7, 8.7 Hz, 1H, Ar-H), 7.64 (d, *J* = 20.0 Hz, 1H, Ar-H), 7.29 (t, *J* = 8.0 Hz, 1H, Ar-H), 5.82 (s, 2H, -OCH₂), 4.21 (q, *J* = 7.0 Hz, 2H, -NCH₂ of -NCH₂CH₃), 1.26 (t, *J* = 7.0 Hz, 3H, -CH₃ of -NCH₂CH₃); ¹³C NMR (101 MHz, DMSO-*d*₆) δ: 172.04 (-CO), 164.76 (-CO), 153.77, 150.92, 142.68 (d, *J* = 20.5 Hz), 136.54, 128.12 (d, *J* = 10.4 Hz), 126.24, 121.06, 113.16 (dd, *J* = 22.7, 15.8 Hz), 110.79, 60.59, 48.13, 14.82; IR (KBr) cm⁻¹: 3079, 1722, 1613, 1520, 1216, 1142, 1040, 840, 762, 603; HRMS (ESI): anal. calcd. For C₂₁H₁₄ClF₃N₄O₃, 462.8132 [M]⁺; found 463.0793 [M + H]⁺.

(1-(4-Chlorophenyl)-1*H*-1,2,3-triazol-4-yl)methyl-7-chloro-1-ethyl-6-fluoro-4-oxo-1,4-dihydroquinoline-3-carboxylate (9e)

Light-pink solid; yield 65 mg (87%); mp: 248–250 °C; ¹H NMR (400 MHz, DMSO-*d*₆) δ: 8.95 (s, 1H, Ar-H), 8.89 (s, 1H, -C=CH of triazole), 8.25 (d, *J* = 6.0 Hz, 1H, Ar-H), 8.04 (d, *J* = 9.3 Hz, 1H, Ar-H), 7.90 (d, *J* = 6.9 Hz, 2H, Ar-H), 7.65 (d, *J* = 7.0 Hz, 2H, Ar-H), 5.85 (s, 2H, -OCH₂), 4.25 (q, *J* = 7.1 Hz, 2H, -NCH₂ of -NCH₂CH₃), 1.29 (t, *J* = 7.1 Hz, 3H, -CH₃ of -NCH₂CH₃); ¹³C NMR (101 MHz, DMSO-*d*₆) δ: 172.10 (-CO), 164.75 (-CO), 150.92, 143.51, 137.93, 136.56, 134.68, 132.12, 129.20, 122.84, 120.73 (d, *J* = 49.3 Hz), 119.30, 113.07 (d, *J* = 22.8 Hz), 110.87, 60.56, 48.55, 14.82; IR (KBr) cm⁻¹: 3093, 1733, 1617, 1488, 1317, 1161, 1042, 781, 674; HRMS (ESI): anal. calcd. For C₂₁H₁₅Cl₂FN₄O₃, 461.2744 [M]⁺; found 461.0609 [M + H]⁺.

(1-(4-Acetylphenyl)-1*H*-1,2,3-triazol-4-yl)methyl-7-chloro-1-ethyl-6-fluoro-4-oxo-1,4-dihydroquinoline-3-carboxylate (9f)

Pale-white solid; yield 49 mg (64%); mp: 190–192 °C; ¹H NMR (600 MHz, DMSO-*d*₆) δ: 9.02 (s, 1H, Ar-H), 8.74 (s, 1H, -C=CH of triazole), 8.23 (d, *J* = 5.8 Hz, 1H, Ar-H), 8.13–8.05 (m, 3H, Ar-H), 7.99 (dd, *J* = 8.8, 4.5 Hz, 2H, Ar-H), 5.41 (s, 2H, -OCH₂), 4.41 (q, *J* = 7.2 Hz, 2H, -NCH₂ of -NCH₂CH₃), 2.62 (s, 3H, -COCH₃),

1.34 (t, *J* = 7.1 Hz, 3H, -CH₃ of -NCH₂CH₃); ¹³C NMR (151 MHz, DMSO-*d*₆) δ: 197.18 (-COCH₃), 171.65 (-CO), 164.03 (-CO), 155.48, 153.84, 150.07, 143.62 (d, *J* = 120.6 Hz), 139.66, 136.27 (d, *J* = 117.0 Hz), 130.26 (d, *J* = 11.5 Hz), 128.87, 125.89 (d, *J* = 19.8 Hz), 123.39, 122.55, 120.55–118.35 (m), 112.79 (d, *J* = 22.5 Hz), 109.38, 57.16, 48.70, 27.04, 14.58; IR (KBr) cm⁻¹: 3132, 2916, 1617, 1596, 1484, 1227, 1157, 1047, 794, 604; HRMS (ESI): anal. calcd. For C₂₃H₁₈ClFN₄O₄, 468.8694 [M]⁺; found 469.1105 [M + H]⁺.

(1-(2-Chloro-4-fluorophenyl)-1*H*-1,2,3-triazol-4-yl)methyl-7-chloro-1-ethyl-6-fluoro-4-oxo-1,4-dihydroquinoline-3-carboxylate (9g)

Pale-yellow solid; yield 50 mg (64%); mp: 224–226 °C; ¹H NMR (400 MHz, DMSO-*d*₆) δ: 8.99 (s, 1H, Ar-H), 8.74 (s, 1H, -C=CH of triazole), 8.31 (d, *J* = 5.7 Hz, 1H, Ar-H), 8.01 (dd, *J* = 20.2, 5.6 Hz, 2H, Ar-H), 7.70 (dd, *J* = 30.3, 8.5 Hz, 1H, Ar-H), 5.87 (s, 2H, -OCH₂), 4.25 (q, *J* = 7.1 Hz, 2H, -NCH₂ of -NCH₂CH₃), 1.30 (t, *J* = 7.1 Hz, 3H, -CH₃ of -NCH₂CH₃); ¹³C NMR (101 MHz, DMSO-*d*₆) δ: 172.10 (-CO), 164.75 (-CO), 156.23, 154.00, 150.92, 143.50, 136.53, 133.86, 129.20, 125.86 (d, *J* = 20.2 Hz), 123.03, 121.58 (d, *J* = 8.2 Hz), 120.98, 118.62 (d, *J* = 22.7 Hz), 113.06 (d, *J* = 22.7 Hz), 110.84, 60.57, 48.50, 14.81; IR (KBr) cm⁻¹: 3090, 2920, 1720, 1612, 1510, 1221, 1026, 794, 714.

(1-(2,3-Dichlorophenyl)-1*H*-1,2,3-triazol-4-yl)methyl 7-chloro-1-ethyl-6-fluoro-4-oxo-1,4-dihydroquinoline-3-carboxylate (9h)

Pale-yellow solid; yield 55 mg (68%); mp: 199–201 °C; ¹H NMR (400 MHz, DMSO-*d*₆) δ: 8.99 (s, 1H, Ar-H), 8.76 (s, 1H, -C=CH of triazole), 8.31 (d, *J* = 6.0 Hz, 1H, Ar-H), 8.04 (d, *J* = 9.3 Hz, 1H, Ar-H), 7.91 (dd, *J* = 8.1, 1.4 Hz, 2H, Ar-H), 7.70 (dd, *J* = 8.0, 1.4 Hz, 2H, Ar-H), 7.59 (t, *J* = 8.1 Hz), 5.89 (s, 2H, -OCH₂), 4.26 (q, *J* = 7.1 Hz, 2H, -NCH₂ of -NCH₂CH₃), 1.30 (t, *J* = 7.1 Hz, 3H, -CH₃ of -NCH₂CH₃); ¹³C NMR (101 MHz, DMSO-*d*₆) δ: 171.97 (-CO), 164.70 (-CO), 156.23, 150.89, 141.84, 132.74, 129.58, 127.82, 127.01, 121.13, 118.92, 113.64, 112.96 (d, *J* = 4.8 Hz), 111.36, 60.58, 48.13, 14.83; IR (KBr) cm⁻¹: 3147, 1685, 1608, 1480, 1229, 1160, 1026, 789.

(1-(4-Nitrophenyl)-1*H*-1,2,3-triazol-4-yl)methyl-7-chloro-1-ethyl-6-fluoro-4-oxo-1,4-dihydroquinoline-3-carboxylate (9i)

Yellow solid; yield 61 mg (80%); mp: 230–232 °C; ¹H NMR (400 MHz, DMSO-*d*₆) δ: 8.95 (s, 1H, Ar-H), 8.89 (s, 1H, -C=CH of triazole), 8.25 (d, *J* = 6.0 Hz, 1H, Ar-H), 8.04 (d, *J* = 9.3 Hz, 1H, Ar-H), 7.90 (d, *J* = 6.9 Hz, 2H, Ar-H), 7.65 (d, *J* = 7.0 Hz, 2H, Ar-H), 5.85 (s, 2H, -OCH₂), 4.25 (q, *J* = 7.1 Hz, 2H, -NCH₂ of -NCH₂CH₃), 1.29 (t, *J* = 7.1 Hz, 3H, -CH₃ of -NCH₂CH₃); ¹³C NMR (101 MHz, DMSO-*d*₆) δ: 171.98 (-CO), 164.70 (-CO), 156.35, 150.93, 143.88, 137.31, 136.58, 135.70, 133.68, 130.37, 122.57 (d, *J* = 34.3 Hz), 121.01, 113.19, 112.99 (d, *J* = 5.9 Hz), 110.85, 60.57, 48.49, 14.83; IR (KBr) cm⁻¹: 3091, 2119, 1720, 1612, 1524, 1338, 1225, 1030, 860, 744.



(1-(3-Chloro-4-fluorophenyl)-1H-1,2,3-triazol-4-yl)methyl 7-chloro-1-((1-(3-chloro-4-fluorophenyl)-1H-1,2,3-triazol-4-yl)methyl)-6-fluoro-4-oxo-1,4-dihydroquinoline-3-carboxylate (10a)

Light-pink solid; yield 103 mg (99%); mp: 228–230 °C; ¹H NMR (600 MHz, DMSO-d₆) δ: 9.03–8.83 (m, 3H, Ar-H, 2 × -C≡CH of triazole), 8.22 (d, *J* = 0.5 Hz, 2H, Ar-H), 8.13 (d, *J* = 1.0 Hz, 1H, Ar-H), 8.06–7.93 (m, 2H, Ar-H), 7.89 (d, *J* = 1.6 Hz, 1H, Ar-H), 7.72–7.55 (m, 2H, Ar-H), 5.87 (s, 2H, -OCH₂), 5.42 (s, 2H, -NCH₂); ¹³C NMR (151 MHz, DMSO-d₆) δ: 165.87 (-CO), 158.00, 152.06, 150.41, 149.69, 148.05, 145.03, 137.85, 137.19, 130.29, 127.71 (d, *J* = 21.6 Hz), 122.94 (d, *J* = 5.1 Hz), 119.76 (d, *J* = 20.1 Hz), 116.79 (d, *J* = 12.4 Hz), 115.02 (d, *J* = 11.9 Hz), 115.29, 115.24, 115.06, 114.92 (d, *J* = 11.1 Hz), 112.51 (d, *J* = 9.7 Hz), 112.36 (d, *J* = 9.8 Hz), 106.87 (d, *J* = 22.5 Hz), 103.86, 51.32, 42.36; IR (KBr) cm⁻¹: 3088, 1734, 1615, 1512, 1223, 1157, 1028, 801, 719.

(1-(3-Chlorophenyl)-1H-1,2,3-triazol-4-yl)methyl-7-chloro-1-((1-(3-chlorophenyl)-1H-1,2,3-triazol-4-yl)methyl)-6-fluoro-4-oxo-1,4-dihydroquinoline-3-carboxylate (10b)

Off-white solid; yield 50 mg (51%); mp: 225–227 °C; ¹H NMR (600 MHz, DMSO-d₆) δ: 9.13–8.82 (m, 3H, Ar-H, 2 × -C≡CH of triazole), 8.22 (s, 1H, Ar-H), 8.08–7.82 (m, 5H, Ar-H), 7.64–7.50 (m, 4H, Ar-H), 5.87 (s, 2H, -OCH₂), 5.44 (s, 2H, -NCH₂); ¹³C NMR (151 MHz, DMSO-d₆) δ: 171.60 (-CO), 163.73 (-CO), 155.40, 153.76, 150.33, 143.60, 142.92, 137.47 (d, *J* = 16.2 Hz), 136.01, 134.21 (d, *J* = 10.8 Hz), 131.63 (d, *J* = 7.4 Hz), 128.66 (d, *J* = 11.6 Hz), 125.47 (d, *J* = 20.0 Hz), 123.32, 122.33, 120.58, 119.94, 118.75 (d, *J* = 6.3 Hz), 112.58 (d, *J* = 22.3 Hz), 109.60, 57.07, 48.12; IR (KBr) cm⁻¹: 3098, 2928, 1734, 1615, 1492, 1218, 1157, 1028, 776, 673.

(1-(4-(Trifluoromethoxy)phenyl)-1H-1,2,3-triazol-4-yl)methyl 7-chloro-6-fluoro-4-oxo-1-((1-(4-(trifluoromethoxy)phenyl)-1H-1,2,3-triazol-4-yl)methyl)-1,4-dihydroquinoline-3-carboxylate (10c)

Off-white solid; yield 55 mg (48%); mp: 210–212 °C; ¹H NMR (600 MHz, DMSO-d₆) δ: 8.96–8.92 (m, 3H, Ar-H, 2 × -C≡CH of triazole), 8.22 (s, 1H, Ar-H), 8.04–7.85 (m, 5H, Ar-H), 7.62–7.52 (m, 4H, Ar-H), 5.87 (s, 2H, -OCH₂), 5.44 (s, 2H, -NCH₂); ¹³C NMR (151 MHz, DMSO-d₆) δ: 172.11 (-CO), 164.33 (-CO), 163.97, 157.25, 156.20, 155.00, 154.22, 153.99, 151.43 (d, *J* = 25.8 Hz), 144.14, 143.47, 136.61, 135.84 (d, *J* = 20.8 Hz), 133.72 (d, *J* = 13.0 Hz), 130.47 (d, *J* = 7.8 Hz), 129.26, 125.55 (d, *J* = 18.2 Hz), 123.80, 122.86, 122.47 (d, *J* = 36.4 Hz), 121.12 (d, *J* = 25.0 Hz), 79.42, 78.25, 57.67, 52.28, 48.67, 43.49; IR (KBr) cm⁻¹: 3103, 2928, 1728, 1610, 1486, 1259, 1213, 1162, 1043, 791.

(1-(2,4-Difluorophenyl)-1H-1,2,3-triazol-4-yl)methyl 7-chloro-1-((1-(2,4-difluorophenyl)-1H-1,2,3-triazol-4-yl)methyl)-6-fluoro-4-oxo-1,4-dihydroquinoline-3-carboxylate (10d)

White solid; yield 88 mg (89%); mp: 227–229 °C; ¹H NMR (600 MHz, DMSO-d₆) δ: 9.04 (s, 1H, Ar-H), 8.71 (m, 2H, 2 × -C≡CH of triazole), 8.34 (d, *J* = 5.2 Hz, 1H, Ar-H), 8.02 (d, *J* = 9.0 Hz, 1H,

Ar-H), 7.97–7.82 (m, 2H, Ar-H), 7.67 (dd, *J* = 21.8, 10.5 Hz, 2H, Ar-H), 7.41–7.28 (m, 2H, Ar-H), 5.87 (s, 2H, -OCH₂), 5.45 (s, 2H, -NCH₂); ¹³C NMR (151 MHz, DMSO-d₆) δ: 171.83 (-CO), 164.15 (-CO), 163.36 (d, *J* = 11.9 Hz), 161.71 (d, *J* = 11.9 Hz), 155.55 (d, *J* = 44.5 Hz), 154.13–153.56 (m), 151.06, 143.22, 142.32, 136.32, 128.94 (d, *J* = 6.4 Hz), 127.93 (dd, *J* = 16.7, 10.2 Hz), 126.75 (d, *J* = 5.0 Hz), 126.05 (d, *J* = 5.5 Hz), 125.78 (d, *J* = 20.0 Hz), 121.91 (d, *J* = 20.9 Hz), 120.94, 113.15 (d, *J* = 5.0 Hz), 113.00 (d, *J* = 5.6 Hz), 112.83, 109.86, 106.19 (d, *J* = 6.6 Hz), 106.11–105.97 (m), 105.85 (d, *J* = 6.7 Hz), 57.36, 48.04; IR (KBr) cm⁻¹: 3078, 1728, 1615, 1522, 1213, 1146, 1043, 842, 606.

(1-(4-Chlorophenyl)-1H-1,2,3-triazol-4-yl)methyl-7-chloro-1-((1-(4-chlorophenyl)-1H-1,2,3-triazol-4-yl)methyl)-6-fluoro-4-oxo-1,4-dihydroquinoline-3-carboxylate (10e)

Off white solid; yield 64 mg (65%); mp: 248–250 °C; ¹H NMR (600 MHz, DMSO-d₆) δ: 9.05–8.97 (m, 3H, Ar-H, 2 × -C≡CH of triazole), 8.28 (s, 1H, Ar-H), 8.10–7.91 (m, 5H, Ar-H), 7.69–7.57 (m, 4H, Ar-H), 5.92 (s, 2H, -OCH₂), 5.50 (s, 2H, -NCH₂); ¹³C NMR (151 MHz, DMSO-d₆) δ: 171.51 (-CO), 163.38 (-CO), 155.42 (d, *J* = 8.0 Hz), 153.78 (d, *J* = 6.5 Hz), 150.85 (d, *J* = 25.8 Hz), 149.85 (d, *J* = 15.0 Hz), 143.57, 142.90, 136.04, 135.26 (d, *J* = 19.1 Hz), 133.15 (d, *J* = 12.8 Hz), 133.15 (d, *J* = 12.8 Hz), 129.90 (d, *J* = 8.1 Hz), 128.69, 125.49 (d, *J* = 19.9 Hz), 123.22 (d, *J* = 4.5 Hz), 122.29 (d, *J* = 4.8 Hz), 122.12–121.62 (m), 120.62 (d, *J* = 6.5 Hz), 112.68 (d, *J* = 5.9 Hz), 112.55, 109.43 (d, *J* = 33.3 Hz), 51.70, 48.10; IR (KBr) cm⁻¹: 3097, 2931, 1731, 1611, 1483, 1313, 1219, 1165, 1045, 780, 671.

(1-(4-Acetylphenyl)-1H-1,2,3-triazol-4-yl)methyl 1-((1-(4-acetylphenyl)-1H-1,2,3-triazol-4-yl)methyl)-7-chloro-6-fluoro-4-oxo-1,4-dihydroquinoline-3-carboxylate (10f)

Light pink solid; yield 97 mg (96%); mp: 258–260 °C; ¹H NMR (600 MHz, DMSO-d₆) δ: 9.04–8.98 (m, 3H, Ar-H, 2 × -C≡CH of triazole), 8.25 (d, *J* = 5.7 Hz, 1H, Ar-H), 8.19–7.94 (m, 6H, Ar-H), 8.03–8.00 (m, 3H, Ar-H), 5.87 (s, 2H, -OCH₂), 5.45 (s, 2H, -NCH₂), 2.62 (d, *J* = 11.9 Hz, 6H, 2 × -COCH₃); ¹³C NMR (151 MHz, DMSO-d₆) δ: 197.19 (-COCH₃), 171.68 (-CO), 164.03 (-CO), 155.26, 153.61, 150.98, 143.97, 143.24, 139.59 (d, *J* = 24.5 Hz), 136.72 (d, *J* = 9.7 Hz), 130.28 (d, *J* = 10.1 Hz), 123.46, 122.55, 120.78, 120.10 (d, *J* = 6.9 Hz), 112.80 (d, *J* = 21.8 Hz), 109.62, 57.25, 48.16, 27.05; IR (KBr) cm⁻¹: 3134, 2918, 1672, 1599, 1486, 1229, 1049, 796, 606; HRMS (ESI): anal. calcd. For C₃₂H₂₃ClFN₇O₅, 640.0284 [M]⁺; found 640.1549 [M + H]⁺.

(1-(2-Chloro-4-fluorophenyl)-1H-1,2,3-triazol-4-yl)methyl-7-chloro-1-((1-(2-chloro-4-fluorophenyl)-1H-1,2,3-triazol-4-yl)methyl)-6-fluoro-4-oxo-1,4-dihydroquinoline-3-carboxylate (10g)

Off-white solid; yield 102 mg (98%); mp: 225–227 °C; ¹H NMR (600 MHz, DMSO-d₆) δ: 9.03 (s, 1H, Ar-H), 8.70 (d, *J* = 29.4 Hz, 2 × -C≡CH of triazole), 8.29 (d, *J* = 5.4 Hz, 1H, Ar-H), 8.03 (d, *J* = 9.1 Hz, 1H, Ar-H), 7.89 (t, *J* = 8.7 Hz, 2H, Ar-H), 7.67 (dd, *J* = 17.7, 7.8 Hz, 2H, Ar-H), 7.58 (dt, *J* = 16.0, 8.0 Hz, 2H, Ar-H), 5.87 (s, -OCH₂), 5.45 (s, -NCH₂); ¹³C NMR (151 MHz, DMSO-d₆) δ: 171.57 (-CO), 163.73 (-CO), 163.02 (d, *J* = 6.7 Hz), 161.35 (d, *J* =



6.3 Hz), 155.31, 153.67, 150.62, 142.42, 141.37, 135.85, 131.09 (d, $J = 5.0$ Hz), 130.91 (d, $J = 4.5$ Hz), 130.01 (dd, $J = 12.5, 7.6$ Hz), 128.53, 126.97, 126.52, 125.43 (d, $J = 19.8$ Hz), 120.57, 117.94 (d, $J = 5.1$ Hz), 117.76 (d, $J = 5.3$ Hz), 115.62 (d, $J = 22.9$ Hz), 112.52 (d, $J = 22.6$ Hz), 109.45, 57.01, 47.81; IR (KBr) cm^{-1} : 3079, 2921, 1730, 1610, 1510, 1381, 1314, 1220, 1024, 800, 763.

(1-(2,3-Dichlorophenyl)-1H-1,2,3-triazol-4-yl)methyl 7-chloro-1-((1-(2,3-dichlorophenyl)-1H-1,2,3-triazol-4-yl)methyl)-6-fluoro-4-oxo-1,4-dihydroquinoline-3-carboxylate (10h)

White solid; yield 101 mg (92%); mp: 198–200 °C; ^1H NMR (600 MHz, DMSO-d_6) δ : 9.03 (s, 1H, Ar-H), 8.70 (d, $J = 29.4$ Hz, $2 \times -\text{C}=\text{CH}$ of triazole), 8.29 (s, 1H, Ar-H), 8.03 (d, $J = 9.1$ Hz, 1H, Ar-H), 7.91 (t, $J = 8.7$ Hz, 2H, Ar-H), 7.67 (dd, $J = 17.7, 7.8$ Hz, 2H, Ar-H), 7.58 (dt, $J = 16.0, 8.0$ Hz, 2H, Ar-H), 5.87 (s, $-\text{OCH}_2$), 5.45 (s, $-\text{NCH}_2$); ^{13}C NMR (151 MHz, DMSO-d_6) δ : 171.58 ($-\text{CO}$), 163.67 ($-\text{CO}$), 155.32, 153.68, 155.32, 153.68, 150.61, 142.46, 141.44, 136.05–135.68 (m), 132.87 (d, $J = 8.0$ Hz), 132.13 (d, $J = 12.0$ Hz), 128.99, 128.49, 127.54 (d, $J = 14.5$ Hz), 127.16 (d, $J = 6.2$ Hz), 126.88, 126.42, 125.44 (d, $J = 19.7$ Hz), 120.58, 112.52 (d, $J = 22.5$ Hz), 109.45, 56.98, 47.78; IR (KBr) cm^{-1} : 3149, 1687, 1610, 1481, 1231, 1162, 1028, 791.

(1-(4-Nitrophenyl)-1H-1,2,3-triazol-4-yl)methyl 7-chloro-6-fluoro-1-((1-(4-nitrophenyl)-1H-1,2,3-triazol-4-yl)methyl)-4-oxo-1,4-dihydroquinoline-3-carboxylate (10i)

Pale-yellow solid; yield 100 mg (98%); mp: 278–280 °C; ^1H NMR (600 MHz, DMSO-d_6) δ : 8.99–8.92 (m, 2H, Ar-H, $-\text{C}=\text{CH}$ of triazole), 8.22 (s, 1H, $-\text{C}=\text{CH}$ of triazole), 8.06–7.99 (m, 2H, ArH), 7.94 (d, $J = 19.8$ Hz, 2H, ArH), 7.85 (s, 2H, ArH), 7.65–7.50 (m, 5H, ArH), 5.87 (s, $-\text{OCH}_2$), 5.44 (s, $-\text{NCH}_2$); ^{13}C -NMR (151 MHz, DMSO-d_6) δ : 171.60 ($-\text{CO}$), 163.73 ($-\text{CO}$), 155.40, 153.76, 150.77, 143.26 (d, $J = 103.2$ Hz), 137.47 (d, $J = 23.4$ Hz), 136.01, 134.21 (d, $J = 10.8$ Hz), 131.63 (d, $J = 7.4$ Hz), 128.66 (d, $J = 11.6$ Hz), 125.40, 123.32, 123.32, 122.33, 120.58, 119.94, 118.75 (d, $J = 6.3$ Hz), 112.58 (d, $J = 22.3$ Hz), 109.60, 57.07, 48.12; IR (KBr) cm^{-1} : 3093, 2120, 1723, 1610, 1522, 1337, 1223, 1028, 858, 744.

X-ray crystallographic analysis

The single-crystal X-ray analysis further verified the structure of synthesized intermediate **6**. Briefly, the crystals were formed *via* the slow evaporation solution technique with ethyl acetate. Graphite monochromatized Cu K α radiation ($\lambda = 1.54184$ Å) was used to measure the X-ray diffraction intensity data at 293 K using the X-ray scan method on a Rigaku XtaLAB Synergy-i single-crystal X-ray diffractometer with a CCD-detector (HyPix-Bantam). The structure of compound **6** was established by the direct method using the Olex2-1.5 software.³⁶ Then, it was refined using the full-matrix least-squares method on F2 by SHELXL.³⁷ Fig. 8 show the thermal ellipsoid plot prepared using ORTEP III³⁸ of compound **6**, which was crystallized in monoclinic system with the $C2/c$ space group. Table 2 provides information about the single-crystal X-ray crystallographic structure of compound **6** (Fig. 9).

Biological assays

Determination of antibacterial activity

The bacterial strains used in the *in vitro* antibacterial investigations included *E. faecalis* (ATCC 29212), *E. faecalis* (clinical isolate), *E. coli* (ATCC 25922), and *E. coli* (clinical isolate). The cultures used in this study were preserved at the Department of Microbiology, Institute of Medical Sciences, Banaras Hindu University, Varanasi, India. All cultures and clinical strains were obtained from the American Type Culture Collection (ATCC). Prior to the screening process, the new microbial broth cultures were prepared in a regular saline solution. The reference medication for evaluating antibacterial effectiveness was ciprofloxacin. The micro-dilution approach was used to calculate the minimum inhibitory concentration (MIC) using a series of dilutions (10-fold) of each chemical.³⁹ In a microtiter plate, the various chemical concentrations were serially diluted. In each tube of the microtiter plate, 10 μL of standardized inoculum ($1-2 \times 10^7$ cfu per mL) was introduced. Subsequently, the plates were incubated for 24 h aerobically at 37 °C. Compared to the wells containing the control, the lowest concentration of the compounds at which they illustrated no sign of bacterial growth and no turbidity in the solution was regarded as the MIC.

Molecular docking

The top selected compounds (**10d** and **9a**) were subjected to molecular docking to understand the fundamental interactions of the compound with the target protein. For the docking studies, the Maestro Suite was used in the Schrodinger software. Docking studies were performed in four steps, as follows: (1) protein preparation, (2) ligand preparation, (3) grid generation, and (4) molecular docking. After molecular docking, the top potent compound (**10d**) complex was subjected to a molecular dynamics (MD) study.

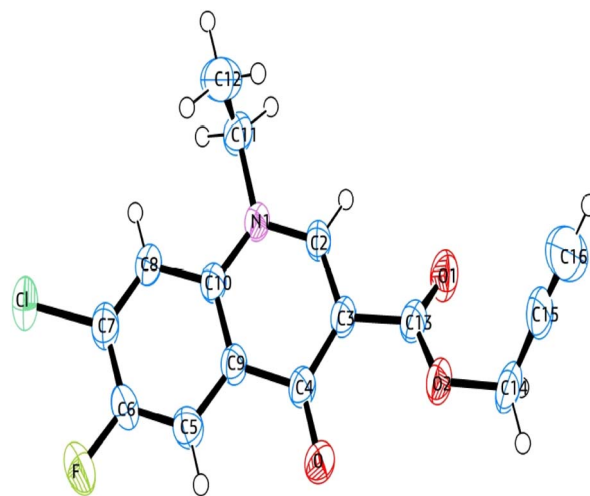


Fig. 8 ORTEP diagram of compound **6** based on single X-ray crystallographic analysis.



Table 2 Crystal data, data collection and structure refinement details for compound **6**

CCDC no.	2345449
Empirical formula	C ₁₅ H ₁₁ ClFNO ₃
Formula weight	307.70
Temperature	293(2) K
Wavelength	1.54184 Å
Crystal system	Monoclinic
Space group	C2/c
Hall group	−C 2yc
Unit cell dimensions	$a = 14.9992(2)$ Å $\alpha = 90$ $b = 9.55020(10)$ Å $\beta = 100.19$ $c = 20.3352(2)$ Å $\gamma = 90$
Volume	$2866.96(6)$ Å ³
Z	8
Density	1.426 g cm ^{−3}
Absorption coefficient	2.561 mm ^{−1}
F(000)	1264.0
Theta range for data collection	8.836 to 144.096
Index ranges	$-17 \leq h \leq 18$ $-11 \leq k \leq 11$ $-25 \leq l \leq 24$
Reflections collected	15 237
Completeness to theta	100%
Absorption correction	Multi-scan
Refinement method	Full-matrix least-squares on F^2
Goodness-of-fit on F^2	1.115
Final R indices [$I > 2$ sigma(I)]	$R_1 = 0.0559$, $wR_2 = 0.1621$

Molecular dynamics (MD) study

Further, the molecular dynamics (MD) study of the selected compound (**10d**) was carried out by using the Desmond Module of the Schrodinger to find the protein–ligand (PL) complex stability.⁴⁰ The PL complex was initially solvated for MD simulation studies with the single point charge solvent model, and

the OPLS2005 force field was used. According to the system builder, the orthorhombic box was selected, and ions and a salt concentration were added to reach the physiological conditions. Next, the energy minimization of the PL complex was done. Then, the MD study was performed for 100 ns with 1.01 bar atmospheric pressure and a temperature of 310 K at the NPT ensemble.⁴¹

DNA gyrase assay

Escherichia coli was grown in 5 mL Luria broth (Himedia) at 37 °C and incubated for 24 h to determine gyrase activity. After incubation of 10 mg mL^{−1} ciprofloxacin, samples **9a** and **10d** 1 mg mL^{−1} were treated with bacterial culture, respectively. Bacterial cells were harvested after 24 h of incubation. A DNA easy (Blood and Tissue) kit from Qiagen (Cat. No. 69504) was used to isolate genomic DNA, and the manufacturer's protocol was followed to isolate the DNA from the control and treated strain. Isolated DNA was checked in 0.8% agarose gel (Amersco, USA) against a 1 kb marker from Fermentas, USA. The DNA was quantified, and its purity was calculated at 260 nm and 280 nm absorbance using a NanoDrop Spectrometer (Thermo Fisher).

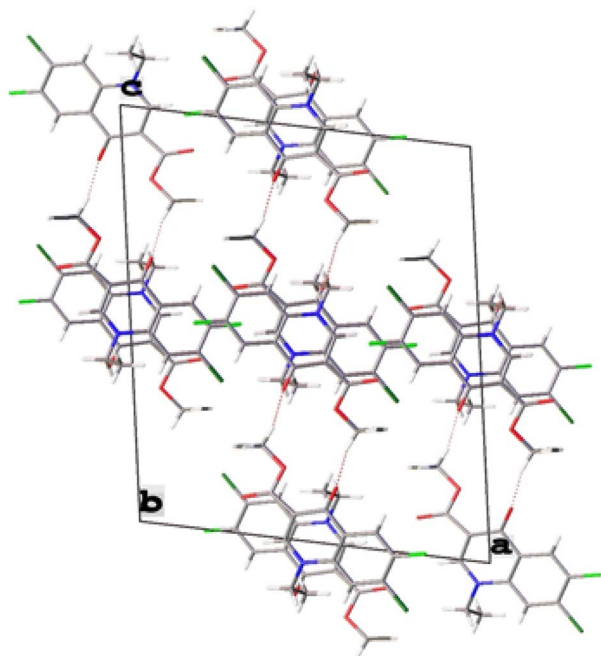
Method of cytotoxicity

The cytotoxicity of the compounds was evaluated in Vero cells (kidney epithelial cells of an African green monkey), using the MTT assay and their CC₅₀ values were calculated. Assays were performed in 96-well microtiter plates, each well containing 100 µL of DMEM medium supplemented with 1% antibiotic solution and 10% fetal bovine serum, and 2×10^4 Vero cells. The cells were treated with varying concentrations (5, 10, 20, 50, 100, and 200 µg mL^{−1}) of each derivative and incubated for 72 h at 37 °C in a CO₂ incubator. After 72 h of incubation, the plates were inspected under an inverted microscope to ensure the growth of the controls and sterile conditions. Then, 10 µL of MTT reagent (5 mg MTT dissolved in 1 mL PBS) was added to each well, and the plates were incubated for 4 h in a cell culture incubator. The formazan crystals formed in each well were dissolved in 100 µL of MTT solubilizing agent (250 µL of 2 M HCl in methanol to 12.5 mL isopropanol) and the absorbance was measured at a wavelength of 590 nm using a SpectraMax iD3 multi-mode microplate reader. The cellular viability in terms of percentage cell survival was calculated as follows:

$$\% \text{ Cell survival} = 100 \times (\text{average OD of treated cells}) / (\text{average OD of control cells}).$$

Conclusions

In total, 20 new synthetic fluoroquinolone 1,2,3-triazole analogues from two series were tested against four different antibacterial stains. Seven compounds from a small library pool, *i.e.*, **7**, **9i**, **10(a–d)**, and **10i**, showed excellent activity

**Fig. 9** Crystal packing of compound **6**.

against *E. coli* (ATCC 25922) strains with MIC of $0.195 \mu\text{g mL}^{-1}$, while compounds **7**, **9a**, and **10(a-d)** showed excellent activity against *E. coli* (clinical isolate), with a MIC of $\geq 0.195 \mu\text{g mL}^{-1}$ and $0.195 \mu\text{g mL}^{-1}$. Moreover, six compounds, *i.e.*, **7**, **9d**, **9i**, **10a**, **10b**, and **10d**, showed excellent activity with MIC in the range of ≥ 0.195 – $0.195 \mu\text{g mL}^{-1}$ against *E. faecalis* (ATCC 29212), whereas the control drug, ciprofloxacin, showed an MIC of $0.781 \mu\text{g mL}^{-1}$. Two compounds, **10a** and **10d**, were found to be more active with an MIC of $6.25 \mu\text{g mL}^{-1}$ compared to the control drug, which showed an MIC of $12.5 \mu\text{g mL}^{-1}$. Further, it was found that electron-withdrawing groups such as OCF_3 , F, Cl, and Br in the benzene ring at the *para*-position played a significant role in defining the antibacterial activity. The cytotoxicity testing results showed that compounds **9a**, **9c**, **10g**, **10h** and **10i** possess toxicity. It is necessary to analyze the structure–activity relationship (SAR) of potential lead molecules and lower their further effective doses while increasing their antibacterial action. Subsequently, the lead molecules from the synthesized compounds should be coupled with current clinical medications to create multifunctional hybrids. This approach will undoubtedly help to reduce the problem of bacterial drug resistance to a certain extent. Moreover, *in silico* studies were performed on the most potent compounds, and it was found that compound **10d** showed the highest docking score of $7.0 \text{ kcal mol}^{-1}$. Thus, due to its highest docking score, it was further subjected to MD analysis with *E. coli* DNA gyrase B complex protein for 100 ns. Also, the *in vitro* assay indicated that **10d** was a more potent inhibitor of DNA gyrase compared to ciprofloxacin employed as a positive control. The single-crystal X-ray analysis of the compounds further confirmed their structure and design criteria. Extensive studies involving a large number of compounds are required to reach any meaningful conclusion in the future.

Data availability

All relevant data are included in the manuscript and its additional files. The data are available from the corresponding author on reasonable request.

Author contributions

Upendra Kumar Patel did the conceptualization, methodology, software, visualization, experimental work, and writing the main text. Alka did the formal analysis and IR data validation. Punit Tiwari did the antibacterial and hemolytic activity under the supervision of Ragini Tilak. Gaurav Joshi and Roshan Kumar did molecular docking studies, molecular dynamic (MD) analysis, DNA gyrase expression assay, software, and visualization. Alka Agarwal supervised, conceptualization, reviewed, and edited the original draft. All authors reviewed the manuscript.

Conflicts of interest

The authors have no conflict of interest regarding manuscript publication.

Acknowledgements

Upendra Kumar Patel is thankful to the Council of Scientific & Industrial Research (CSIR) HRDG New Delhi, India (Grant No. 09/013(0933)/2020-EMR-I) for the Junior Research Fellowship and Senior Research Fellowship. Alka is thankful to CSIR-UGC, New Delhi, India, for providing the Junior Research Fellowship and Senior Research Fellowship (Award Ref. No. 105/(CSIR-UGC NET JUNE 2019)). Alka Agarwal is thankful to Banaras Hindu University and the Institute of Eminence (IoE No. Dev Scheme No 6031), Varanasi, India, for the financial support. The authors are also thankful to CDC-Banaras Hindu University, India, for providing instrumentation facilities.

References

- 1 P. Dadgostar, Antimicrobial Resistance: Implications and Costs, *Infect. Drug Resist.*, 2019, **12**, 3903–3910.
- 2 C. Llor and L. Bjerrum, Antimicrobial resistance: risk associated with antibiotic overuse and initiatives to reduce the problem, *Ther. Adv. Drug Saf.*, 2014, **5**, 229–241.
- 3 L. Rigottier-Gois, C. Madec, A. Navickas, R. C. Matos, E. Akary-Lepage, M. Y. Mistou and P. Serron, The Surface RhamnopolysaccharideEpa of *Enterococcus faecalis* Is a Key Determinant of Intestinal Colonization, *J. Infect. Dis.*, 2015, **211**, 62–71.
- 4 (a) Z. Chen, K. Song, Y. P. Shang, Y. P. Xiong, Z. H. Lyu, J. W. Chen, J. X. Zheng, P. Y. Li, Y. Wu, C. J. Gu, Y. H. Xie, Q. W. Deng, Z. J. Yu, J. Zhang and D. Qu, Selection and Identification of Novel Antibacterial Agents against Planktonic Growth and Biofilm Formation of *Enterococcus faecalis*, *J. Med. Chem.*, 2021, **64**, 15037–15052; (b) S. Manoharadas, M. Altaf, N. Ahmad, A. F. Alrefaei and B. F. Al-Rayes, Construction and Activity Testing of a Modular Fusion Peptide against *Enterococcus faecalis*, *Antibiotics*, 2023, **12**, 388.
- 5 (a) X. M. Zhou, Y. Y. Hu, B. Fang and C. H. Zhou, Benzenesulfonylthiazoloimines as unique multitargeting antibacterial agents towards *Enterococcus faecalis*, *Eur. J. Med. Chem.*, 2023, **248**, 115088; (b) A. A. Iannetta, N. E. Minton, A. A. Uitenbroek, J. L. Little, C. R. Stanton, C. J. Kristich and L. M. Hicks, IreK-Mediated, Cell Wall-Protective Phosphorylation in *Enterococcus faecalis*, *J. Proteome Res.*, 2021, **20**, 5131–5144.
- 6 C. Muller, S. Massier, Y. L. Breton and A. Rince, The role of the CroR response regulator in resistance of *Enterococcus faecalis* to D-cycloserine is defined using an inducible receiver domain, *Mol. Microbiol.*, 2018, **107**, 416–427.
- 7 E. Ruppe, P.-L. Woerther and F. Barbier, Mechanisms of antimicrobial resistance in Gram-negative bacilli, *Ann. Intensive Care*, 2015, **5**, 21–36.
- 8 World Health Organization, *Prioritization of pathogens to guide discovery, research and development of new antibiotics for drug-resistant bacterial infections, including tuberculosis*, 2017(WHO/EMP/IAU/2017.12), WHO, Geneva, Switzerland, 2017.



- 9 J. A. Mohamed and D. B. Huang, Biofilm formation by enterococci, *J. Med. Microbiol.*, 2007, **56**, 1581–1588.
- 10 O. Tenaillon, D. Skurnik, B. Picard and E. Denamur, The population genetics of commensal *Escherichia coli*, *Nat. Rev. Microbiol.*, 2010, **8**, 207–217.
- 11 E. Jimenez, M. L. Marin, R. Martin, J. M. Odriozola, M. Olivares, J. Xaus, L. Fernandez and J. M. Rodriguez, Is meconium from healthy newborns actually sterile?, *Res. Microbiol.*, 2008, **159**, 187–193.
- 12 M. I. Andersson and A. P. MacGowan, Development of the quinolones, *J. Antimicrob. Chemother.*, 2003, **51**, 1–11.
- 13 A. L. Aguirre, P. R. Chheda, S. R. C. Lentz, H. A. Held, N. P. Groves, H. Hiasa and R. J. Kerns, Identification of an ethyl 5,6-dihydropyrazolo[1,5-c]quinazoline-1-carboxylate as a catalytic inhibitor of DNA gyrase, *Bioorg. Med. Chem.*, 2020, **28**, 115439.
- 14 E. N. Esfahani, M. Mohammadi-Khanaposhtani, Z. Rezaei, Y. Valizadeh, R. Rajabnia, M. Hassankalhor, F. Bandarian, M. A. Faramarzi, N. Samadi, M. R. Amini, M. Mahdavi and B. Larijani, New ciprofloxacin-dithiocarbamate-benzyl hybrids: design, synthesis, antibacterial evaluation, and molecular modeling studies, *Res. Chem. Intermed.*, 2019, **45**, 223–236.
- 15 Z. Xu, S. J. Zhao, Z. S. Lv, F. Gao, Y. Wang, F. Zhang, L. Bai and J. L. Deng, Fluoroquinolone-isatin hybrids and their biological activities, *Eur. J. Med. Chem.*, 2019, **162**, 396–406.
- 16 R. J. Reece and A. Maxwell, DNA gyrase: structure and function, *Crit. Rev. Biochem. Mol. Biol.*, 1991, **26**, 335–375.
- 17 V. V. Rostovtsev, L. G. Green, V. V. Fokin and K. B. Sharpless, A Stepwise Huisgen Cycloaddition Process: Copper(I)-Catalyzed Regioselective “Ligation” of Azides and Terminal Alkynes, *Angew. Chem., Int. Ed.*, 2002, **41**, 2596.
- 18 H. C. Kolb and K. B. Sharpless, The growing impact of click chemistry on Drug Discovery, *Drug Discovery Today*, 2003, **8**, 1128.
- 19 S. G. Agalave, S. R. Maujan and V. S. Pore, Click Chemistry: 1,2,3-Triazoles as Pharmacophores, *Chem.-Asian J.*, 2011, **6**, 2696.
- 20 R. Huisgen, G. Szeimies and L. Mobius, 1,3-Dipolare Cycloadditionen, XXXII. Kinetik der Additionenorganischer Azide an CC-Mehrfachbindungen, *Chem. Ber.*, 1967, **100**, 2494–2507.
- 21 A. Massarotti, S. Aprile, V. Mercalli, E. D. Grosso, G. Grosa, G. Sorba and G. C. Tron, Are 1,4- and 1,5-disubstituted 1,2,3-triazoles good pharmacophoric groups?, *ChemMedChem*, 2014, **9**, 2497–2508.
- 22 S. G. Agalave, S. R. Maujan and V. S. Pore, Click Chemistry: 1,2,3-Triazoles as Pharmacophores, *Chem.-Asian J.*, 2011, **6**, 2696–2718.
- 23 D. Gonzalez-Calderon, M. G. Mejía-Dionicio, M. A. Morales-Reza, A. Ramirez-Villalva, M. Morales-Rodríguez, B. Jauregui-Rodríguez, E. Díaz-Torres, C. Gonzalez-Romero and A. Fuentes-Benites, Azide-enolate 1,3-dipolar cycloaddition in the synthesis of novel triazole-based miconazole analogues as promising antifungal agents, *Eur. J. Med. Chem.*, 2016, **112**, 60–65.
- 24 R. Kant, V. Singh, G. Nath, S. K. Awasthi and A. Agarwal, Design, synthesis and biological evaluation of ciprofloxacin tethered bis-1,2,3-triazole conjugates as potent antibacterial agents, *Eur. J. Med. Chem.*, 2016, **124**, 218–228.
- 25 M. K. Singh, R. Tilak, G. Nath, S. K. Awasthi and A. Agarwal, Design, synthesis and antimicrobial activity of novel benzothiazole analogs, *Eur. J. Med. Chem.*, 2013, **63**, 635–644.
- 26 A. Agarwal, P. Singh, A. Maurya, U. K. Patel, A. Singh and G. Nath, Ciprofloxacin-Tethered 1,2,3-Triazole Conjugates: New Quinolone Family Compounds to Upgrade Our Antiquated Approach against Bacterial Infections, *ACS Omega*, 2022, **7**, 2725–2736.
- 27 U. K. Patel, P. Tiwari, R. Tilak, G. Joshi, R. Kumar and A. Agarwal, Synthesis of ciprofloxacin-linked 1,2,3-triazole conjugates as potent antibacterial agents using click chemistry: exploring their function as DNA gyrase inhibitors *via in silico*- and *in vitro*-based studies, *RSC Adv.*, 2024, **14**, 17051.
- 28 F. Ushiyama, H. Amada, Y. Mihara, T. Takeuchi, N. Tanaka-Yamamoto, M. Mima, M. Kamitani, R. Wada, Y. Tamura, M. Endo, A. Masuko, I. Takata, K. Hitaka, H. Sugiyama and N. Ohtake, Lead optimization of 8-(methylamino)-2-oxo-1,2-dihydroquinolines as bacterial type II topoisomerase inhibitors, *Bioorg. Med. Chem.*, 2020, **28**, 115776.
- 29 P. Price and T. J. McMillan, Use of the tetrazolium assay in measuring the response of human tumor cells to ionizing radiation, *Cancer Res.*, 1990, **50**, 1392–1396.
- 30 P. Singh, C. Sharma, B. Sharma, A. Mishra, D. Agarwal, D. Kannan, J. Held, S. Singh and S. K. Awasthi, N-sulfonylpiperidinedispiro-1,2,4,5-tetraoxanes exhibit potent *in vitro* antiplasmodial activity and *in vivo* efficacy in mice infected with P. berghei ANKA, *Eur. J. Med. Chem.*, 2022, **15**, 114774.
- 31 H. Koga, A. Itoh, S. Murayama, S. Suzue and T. Irikura, Structure-activity relationships of antibacterial 6,7- and 7,8-disubstituted 1-alkyl-1,4-dihydro-4-oxoquinoline-3-carboxylic acids, *J. Med. Chem.*, 1980, **23**, 1358–1363.
- 32 S. K. Dixit, N. Mishra, M. Sharma, S. Singh, A. Agarwal, S. K. Awasthi and V. K. Bhasin, Synthesis and *in vitro* antiplasmodial activities of fluoroquinolone analogs, *Eur. J. Med. Chem.*, 2012, **51**, 52–59.
- 33 J. C. Mc Pherson III, R. Runner, T. B. Buxton, J. F. Hartmann, D. Farcasiu, I. Bereczki, E. Roth, S. Tollas, E. Ostorházi, F. Rozgonyi and P. Herczegh, Synthesis of osteotropic hydroxybisphosphonate derivatives of fluoroquinolone antibacterials, *Eur. J. Med. Chem.*, 2012, **47**, 615–618.
- 34 M. Hu, J. Li and S.-Q. Yao, In situ “click” assembly of small molecule matrix metalloprotease inhibitors containing zinc-chelating groups, *Org. Lett.*, 2008, **10**, 5529–5531.
- 35 H. C. Kolb, M. G. Finn and K. B. Sharpless, Click Chemistry: Diverse Chemical Function from a Few Good Reactions, *Angew. Chem., Int. Ed.*, 2001, **40**, 2004–2021.
- 36 O. V. Dolomanov, L. J. Bourhis, R. J. Gildea, J. A. K. Howard and H. Puschmann, iotbx.cif: a comprehensive CIF toolbox, *J. Appl. Crystallogr.*, 2009, **42**, 339–341.



- 37 G. M. Sheldrick, SHELXT-Integrated Space-Group and Crystal-Structure Determination, *Acta Crystallogr., Sect. A*, 2015, **71**, 3–8.
- 38 L. J. Farrugia, WinGX and ORTEP for Windows: An Update, *J. Appl. Crystallogr.*, 2012, **4**, 5849–5854.
- 39 S. F. Nielsen, M. Larsen, T. Boesen, K. Schønning and H. Kromann, Cationic Chalcone Antibiotics. Design, Synthesis, and Mechanism of Action, *J. Med. Chem.*, 2005, **48**, 2667–2677.
- 40 P. Vishwakarma, N. F. Siddiqui, S. Thakur and H. Jadhav, FDA approved fused-pyrimidines as potential PI3K inhibitors: a computational repurposing approach, *J. Biomol. Struct. Dyn.*, 2023, 1–18, DOI: [10.1080/07391102.2023.2276315](https://doi.org/10.1080/07391102.2023.2276315).
- 41 S. A. Hollingsworth and R. O. Dror, Molecular Dynamics Simulation for All, *Neuron*, 2018, **99**, 1129–1143.

